NATIONAL AERONAUTICS AND SPACE ADMINISTRATION

Technical Report No. 32-666

A Figure of Merit Measuring Picture Resolution

T. Rindfleisch
D. Willingham

JET PROPULSION LABORATORY
CALIFORNIA INSTITUTE OF TECHNOLOGY
PASADENA, CALIFORNIA

September 1, 1965

NATIONAL AERONAUTICS AND SPACE ADMINISTRATION

Technical Report No. 32-666

A Figure of Merit Measuring Picture Resolution

T. Rindfleisch
D. Willingham

H. G. Trostle, *Manager*
Space Instruments Section

JET PROPULSION LABORATORY
CALIFORNIA INSTITUTE OF TECHNOLOGY
PASADENA, CALIFORNIA

September 1, 1965

Prepared Under Contract No. NAS 7-100
National Aeronautics & Space Administration

CONTENTS

FIGURES

FIGURES (Cont'd)

ABSTRACT

In order to optimize the quality of data obtained from lunar and planetary photographic missions, a general and versatile resolution measure is needed that accounts for the numerous degrading factors inherent in the facsimile system. A mathematical formalism is developed which leads to a single number or figure of merit measuring a characteristic dimension of the smallest detectable object in a picture of an extended complex scene. The formalism is in modular form and can include the effects on the system resolution due to statistical and photometric properties of the surface being viewed, atmospheric turbulence, image motion, characteristics of the television and recording system, system noises, and properties of the human observer. The treatment is unified within the framework of linear system analysis and assumes that portions of the transfer process act as spatial filters and that the human observer functions as a signal-to-noise optimizing low-pass filter. The contrast present in the object scene is determined by the statistical and photometric properties of the scene. A comparison of the figure of merit to conventional resolution measures is made, indicating its advantages for system design and performance evaluation over the conventional engineering comparison techniques, which do not predict absolute performance.

Author

I. INTRODUCTION

The purpose of this Report is to determine a single number or figure of merit characterizing the picture resolution expected from a spacecraft visual system. It is to be a measure of a characteristic dimension of the smallest typical object just detectable by an observer viewing the object scene reproduction. The calculation is to include the effects of the spacecraft environment and object scene contrast characteristics as related to picture quality. In the following Sections, a suitable resolution measure is formulated and expressed as a function of viewing geometry, object scene photometric characteristics, inherent facsimile system characteristics, system noise, image motion and similar degrading effects, and the capabilities of a human observer. The need for such a tool is evident in light of the problem at hand, namely, the optimization of the quality of the picture data obtained by a spacecraft with respect to mission variables.

Conventional resolution measures are inadequate in the present context. The usual approach is to determine the

limiting spatial frequency such that a set of light and dark bars of fixed contrast is just resolvable through the system. This approach has its principal value in engineering evaluations and comparisons of systems but is hardly an aid to the solution of the present problem.

Thus, the figure of merit is intended as a complete and versatile measure of the resolution capabilities of a system when viewing a complex, extended scene. In particular, it has been applied to the *Ranger* impacting television mission as a tool in determining, from the standpoint of picture quality and resolution, optimal approach trajectories and impact areas before and during spacecraft flight operations. The analysis presented here, however, is general in nature and can be applied to a wide variety of imaging systems and problems.

II. DEFINITION OF THE FIGURE OF MERIT

The purpose of lunar spacecraft television systems is, of course, the acquisition of lunar surface information. The single number or figure of merit defined here is intended as a measure of the overall capability of a television system to accomplish this goal as a function of system characteristics, trajectory, viewing geometry, and lunar photometric properties. This capability is predicated almost entirely on the ability of a human observer to detect and recognize objects and features on the lunar surface from the system reproduction of the scene being viewed. Thus, to define an appropriate criterion, one must understand the meaning of "detection" and "recognition" for the human observer.

Detection is a rather straightforward concept allowing simple quantitative description. Detection of something in a picture implies cognizance of detail other than a uniform background plus random noise without necessarily knowing exactly what it is. Thus, it is required simply that the particular detail of interest have sufficient contrast with the background to be lifted out of the background noise. That is, for a given detail to be detectable, it must have a signal to root-mean-square (rms) noise ratio greater than some predictable value.

Recognition is a far more nebulous and subjective concept, for which a satisfactory quantitative description has not been found. It implies a complex correlation of what the observer sees with his past experience and bias to the end of properly cataloging the new information he is receiving. The problem to be concerned with here is whether or not the image information the observer receives will give him, after he processes it, an accurate representation of the actual object scene being viewed. The variety of shapes in nature is myriad, and just how the luminance gradients in the image the observer views must correlate with the surface curvatures of the actual object for proper interpretation is indeed unknown and must be a complicated function of the observer's background experience, among other factors. Thus, at this time, there is no quantitative way of predicting whether or not a particular object being viewed will be properly recognized by an observer from the system reproduction of the scene, much less what the threshold for such recognition might be as a function of viewing geometry, system parameters, and image blur.

An approximate approach to circumvent this dilemma would be to postulate that the threshold size for recognition of an object under given conditions has to be a certain number of times larger than the threshold size for detection under the same conditions. The magnitude of this coefficient is certainly not obvious *a priori* and undoubtedly varies with the set of objects under consideration. This approach is currently under investigation by the authors, but no results are available yet.

With the ideas of detection and recognition in mind, then, a measure of system resolution in terms of the ability of an observer to detect relief surface features against a uniform background can be formulated. Adopting and extending Schade's idea (Ref. 1), a *resolution element* is defined as the smallest square on the lunar surface with representative contrast with the background which, when viewed in the system reproduction, produces a signal-to-rms-noise ratio of 3 for the observer. The value of 3 for the threshold signal-to-noise ratio is taken from Schade's work but is currently being re-evaluated experimentally in the present context.

To specify the contrast of the resolution element with the uniform background, one must consider the origin of this contrast. Assuming homogeneous surface properties, it arises in two ways. First, various portions of the surface of a relief feature have different orientations with respect to the light source and the observer than does the background and, hence, different luminance values. Second, the shadow cast by a relief feature makes an important contrast contribution. For the present purposes, a measure of the contrast between a point on the surface of a relief feature or in its shadow and the uniform background is taken to be the magnitude of the difference in their luminances.

Since, in this approximation, the resolution element is clearly intended to be representative of small surface features ("small," implying on the order of the resolution limits of the system), the appropriate value of its contrast should be some sort of average over the contrasts occurring about the surface and in the shadow of an "average" lunar feature. Note that the choice of a resolution element with uniform luminance to represent complex surface features is not unrealistic at the limits of system resolution in the detection sense, since the details of the more complicated luminance distribution for the real object will be largely obscured. The averaging process should use as its weighting function area elements as projected into the image plane on the face of the camera sensor tube. This choice is made because the observer sees a reproduction of this projection of the object scene and from it, extracts what information he can. In the selection of a representative lunar feature from which to derive an average contrast, one has no knowledge of lunar surface statistics on the scale of the expected resolution limits of the *Ranger* camera systems. It is felt, however, that a right-circular cone whose surface has the lunar photometric properties offers a promising model if its base angle is chosen to correspond to observed lunar characteristics. A conical shape appears useful because it seems intuitively quite representative of features found on the Moon on a larger scale—both protuberances and depressions. Furthermore, a cone has no preferred surface orientation azimuthally about its axis, and such isotropy with respect to azimuth about the local surface normal is expected, on the average, to exist on the Moon. While this isotropy holds for any symmetrical object, the cone is probably the simplest for this application.

Now, to determine an appropriate value for the cone base angle, it is noted that Kopal (Ref. 2), among others, has estimated from visual and radar observations of the Moon that the surface has a mean slope of 15 deg or less with the local horizontal. No estimates of variations about this mean are given, but certainly much steeper and more gradual slopes are expected. For the present purposes, however, the value of 15 deg will be taken as representative. It is instructive, of course, to investigate a system's performance when viewing various features from slopes of, say, 5 up to 45 deg with the horizontal.

The resolution-element contrast with the background, then, for a particular point on the lunar surface will be determined by averaging the magnitude of the object-to-background luminance difference over the images of an upright and an inverted 15-deg base-angle cone located at that point. This will include the contrast effects of both protrusion- and depression-type features. The average is calculated separately over those regions of the image which are brighter than the background and those regions, including the shadow, which are darker than the background. This distinction is made because the system must respond with opposite signals for each, so that their respective contrast contributions should not be considered strictly equivalent.

Thus, both light and dark resolution elements are considered, the sizes of which are determined by requiring that their images, when processed through the television system, produce signal-to-rms-noise ratios of 3 for an observer. The television process includes any degrading factors such as image motion and bandwidth limitations. Threshold-detectable cone diameters are determined by requiring the average (over upright and inverted cones) of lighter-than-background and darker-than-background image areas of the cones to equal the image areas of the light and dark resolution elements, respectively. The figure of merit is then defined as the effective threshold-detectable cone diameter. The reciprocal of this effective diameter is taken to be equal to the sum of the reciprocals of the threshold-detectable cone diameters determined for lighter-than-background and darker-than-background contrasts. Note that this addition law is an attempt to measure the interaction between highlight and shadow areas. That is, if an object feature displays both light and dark areas, it is more easily detectable than if it had only a light area or a dark area. However, if, for example, a feature must be much larger for its light portion to be detectable than its dark portion, the threshold detection would be made almost completely from the dark portion. In the opposite case, the threshold detection is made from the light portion. These effects are inherent in the above addition law.

It should be noted that with the assumption of a homogeneous lunar surface, the figure of merit defined here is a measure of the sizes of *relief surface detail* resolvable

through the system. Inhomogeneities certainly exist in the photometric properties of the lunar surface, but detection of such features is dependent upon their nature and statistical distribution and is not touched upon by the present figure of merit.

It is felt that the figure of merit as defined above provides a very useful indicator of the performance capabilities of a spacecraft television system in terms of resolution. It incorporates the effects of the environment in which the system must operate, the nature of the scene being viewed, the system's inherent parameters, and the human observer's capabilities into a measure of the smallest objects detectable in the scene being viewed. Although it is expected that the numbers resulting from a calculation of the figure of merit have meaning in their absolute magnitude, errors in the photometric property data or in other necessary experimentally obtained data could cause deviations. The usefulness of the figure of merit does not lie solely in its absolute magnitude, however. The variation of its value as a function of position on the lunar surface can be used to optimize the choice of impact point or trajectory from the standpoint of *relative* resolution capabilities. That is, one chooses as the optimum viewing or impact point the position at which the figure of merit reaches a minimum. That it does reach a minimum value at some point on the lunar surface for a given family of trajectories will be seen later. In its application to the *Ranger* impacting spacecraft, this feature of the figure of merit concept proved extremely useful.

III. DESCRIPTION OF SYSTEM ANALYSIS APPROACH

Having defined the quantity of interest, the figure of merit, it remains to elucidate a mathematical approach to its calculation in general. That is, a quantitative description must be formulated for the viewing geometry, the lunar photometric properties, the spacecraft television and recording system as a whole, the effects of image blur, and the capabilities of the human observer.

A. Viewing Geometry

For the purpose of describing the viewing geometry, a *Moon-centered coordinate system* is defined as follows. Let the plane containing the mean Earth–Moon line and the mean Sun–Moon line be the xy-plane of a right-handed Cartesian coordinate system with its origin at the center of the Moon. Let the mean Earth–Moon line be along the positive x-axis, and let the direction of the component of the lunar spin vector normal to the xy-plane define the positive z-axis (see Fig. 1).

The notation will be adopted that an arbitrary vector in the Moon-centered coordinate system is written $\mathbf{V}$ and a unit vector in the same direction is written $\hat{\mathbf{V}}$.

The spacecraft is located in this coordinate system with the following vector definitions, where O is the observed point of interest on the lunar surface (see Fig. 1):

$\hat{\mathbf{x}}, \hat{\mathbf{y}}, \hat{\mathbf{z}}$ unit vectors along the principal Cartesian directions

$\hat{\mathbf{R}}_{MS}$ unit vector from the Moon's center to the Sun's center

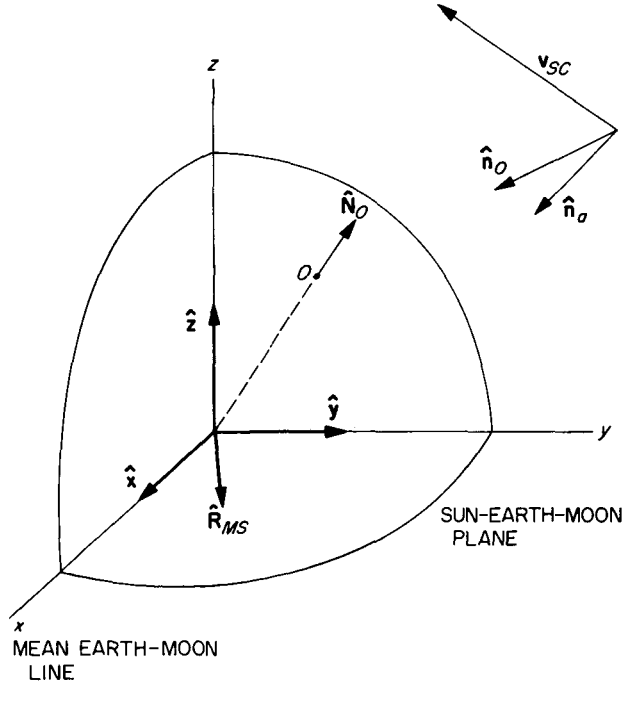

Fig. 1. Vector definitions

$\hat{\mathbf{N}}_O$ unit normal to the spherical lunar surface at point O

$\hat{\mathbf{n}}_O$ unit vector from the spacecraft camera to point O

$\hat{\mathbf{n}}_a$ unit vector along the spacecraft camera optical axis

v_{SC} velocity vector of the spacecraft with respect to the Moon-centered coordinate system

With these coordinate-system and vector definitions, the relative trajectory, illumination, observation, and surface normal geometry can be described. The definitions will be drawn upon freely in the following Sections.

B. Lunar Reflectivity Properties

The following lunar reflectivity properties are based on a report by Eimer (Ref. 3) summarizing the results of a reflectivity study of the Moon by Herriman, Washburn, and Willingham (Ref. 4). It is pointed out that the present level of knowledge is founded solely on Earth-based observations of lunar maria. Thus, one has information only about the average reflective properties of selected areas which are relatively large compared with those presumably resolvable through spacecraft television systems. It must therefore be assumed that the lunar surface is covered with a photometrically homogeneous material having the average properties found in the mare regions.

The Moon's reflective characteristics are quantitatively described by the lunar reflectance function, which is the reflectance coefficient of the surface as a function of incidence angle i, emission angle e, and phase angle g (see Fig. 2). That is, the surface luminance as a function of the photometric geometry is given by the expression

$$b(i, e, g) = E_0 \rho(i, e, g)^* \tag{1}$$

where $b(i, e, g)$ is the surface luminance in foot-lamberts, E_0 is the mean solar constant at the Moon's surface in lumens per square foot (foot-candles), and $\rho(i, e, g)$ is the reflectance function of the surface.

*In Ref. 4, the notation $\rho(i, e, g) = \rho_0\phi(i, e, g)$ is used, where ρ_0 is the full-Moon albedo or reflectance coefficient for normal incidence and emission and $\phi(i, e, g)$ is the surface photometric function normalized such that $\phi(0, 0, 0) \equiv 1$.

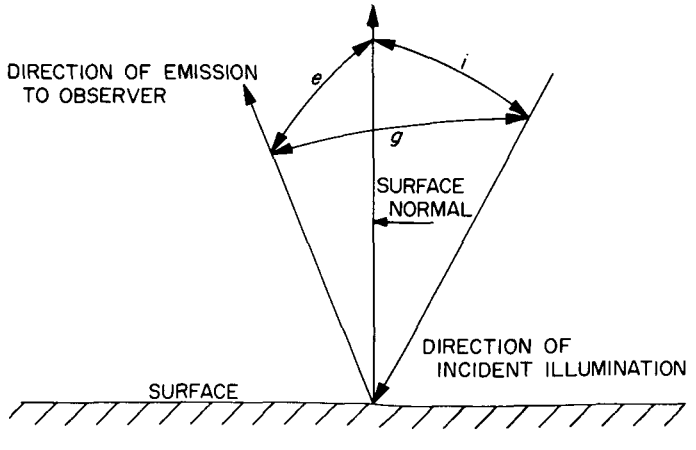

Fig. 2. Photometric angles

It is further pointed out that because of special observed properties of the lunar surface, the reflectance function can be written as a function of only two angles, g and α. The angle g is still the phase angle and α is the projection of the emission angle e in the plane containing the directions of incidence and emission. Note that α is considered positive if its areal sector ($\leq \pi/2$) does not overlap the areal sector ($\leq \pi$) between the incidence and emission directions and is considered negative otherwise (see Fig. 3).

Figure 4 shows the resultant reflectance function from the most recent compilation of available data by Willingham (Ref. 5).

The photometric angles introduced above can be expressed in terms of the spacecraft viewing geometry (see Fig. 1) as follows. In Moon-centered coordinates, the direction of incidence, neglecting parallax, is $-\hat{\mathbf{R}}_{MS}$ and the direction of emission is $-\hat{\mathbf{n}}_O$. Then, letting the surface of interest have unit normal $\hat{\mathbf{N}}$, the angles are

$$\begin{aligned} i &= \arccos(\hat{\mathbf{N}}\cdot\hat{\mathbf{R}}_{MS}), \quad O \leq i \leq \pi/2 \\ e &= \arccos(-\hat{\mathbf{N}}\cdot\hat{\mathbf{n}}_O), \quad O \leq e \leq \pi/2 \\ g &= \arccos(-\hat{\mathbf{n}}_O\cdot\hat{\mathbf{R}}_{MS}), O \leq g \leq \pi \end{aligned} \tag{2}$$

To express the angle α similarly, consider Fig. 5. Let $\hat{\mathbf{A}}$ be a unit normal to the plane containing the incidence and emission directions. That is, let

$$\hat{\mathbf{A}} = \frac{\hat{\mathbf{n}}_O \times \hat{\mathbf{R}}_{MS}}{|\hat{\mathbf{n}}_O \times \hat{\mathbf{R}}_{MS}|}, \qquad |\hat{\mathbf{n}}_O \times \hat{\mathbf{R}}_{MS}| \neq 0$$

Note that the case for which $|\hat{\mathbf{n}}_O \times \hat{\mathbf{R}}_{MS}| = 0$ is the case in which the phase angle equals zero or π. The symmetries imposed by assuming that the reflectance function can be written as a function of g and α also require that for $g = 0$, ρ must be a constant independent of α. This is intimately connected with the fact that the definition of α loses all meaning for the zero phase-angle case. The case in which $g = \pi$ is that of glancing incidence and emission, for which ρ will be taken as zero by definition. Avoiding these situations as trivial, the unit vector $\mathbf{N}_1$ in the direction of the component of $\mathbf{N}$ in the plane containing the incidence and emission directions can be written as

$$\hat{\mathbf{N}}_1 = \frac{\hat{\mathbf{N}} - \hat{\mathbf{A}}(\hat{\mathbf{N}}\cdot\hat{\mathbf{A}})}{|\hat{\mathbf{N}} - \hat{\mathbf{A}}(\hat{\mathbf{N}}\cdot\hat{\mathbf{A}})|} = \frac{\hat{\mathbf{A}} \times (\hat{\mathbf{N}} \times \hat{\mathbf{A}})}{|\hat{\mathbf{N}} \times \hat{\mathbf{A}}|}, \qquad |\hat{\mathbf{N}} \times \hat{\mathbf{A}}| \neq 0$$

Note again that the case for which $|\hat{\mathbf{N}} \times \hat{\mathbf{A}}| = 0$ is one in which the definition of α loses its meaning and corresponds to glancing incidence and emission, another trivial case. So, avoiding it, the angle α can be written with the proper sign as

$$\sin\alpha = [(\hat{\mathbf{N}}_1 \times \hat{\mathbf{n}}_O)\cdot\hat{\mathbf{A}}], \qquad -\frac{\pi}{2} \leq \alpha \leq \frac{\pi}{2}$$

Expanding the right side, one obtains

$$\sin\alpha = \frac{(\hat{\mathbf{n}}_O\cdot\hat{\mathbf{R}}_{MS})(\hat{\mathbf{n}}_O\cdot\hat{\mathbf{N}}) - (\hat{\mathbf{R}}_{MS}\cdot\hat{\mathbf{N}})}{[(\hat{\mathbf{n}}_O\cdot\hat{\mathbf{N}})^2 + (\hat{\mathbf{R}}_{MS}\cdot\hat{\mathbf{N}})^2 - 2(\hat{\mathbf{n}}_O\cdot\hat{\mathbf{N}})(\hat{\mathbf{R}}_{MS}\cdot\hat{\mathbf{N}})(\hat{\mathbf{n}}_O\cdot\hat{\mathbf{R}}_{MS})]^{1/2}}$$

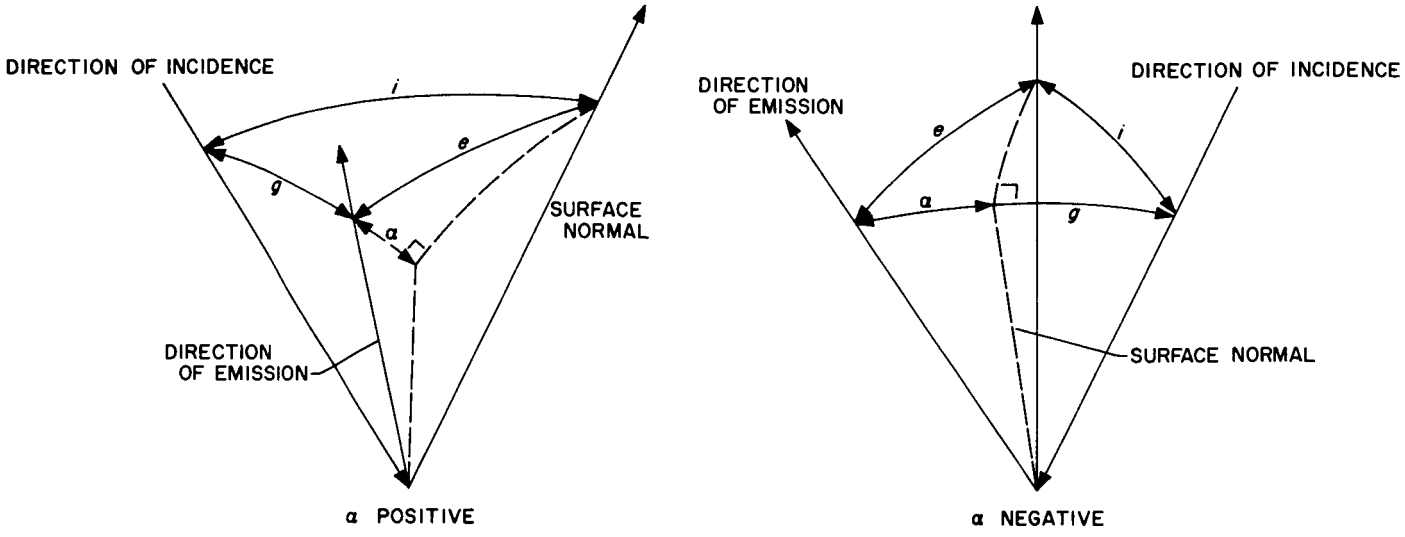

Fig. 3. Definition and sign convention for the angle α

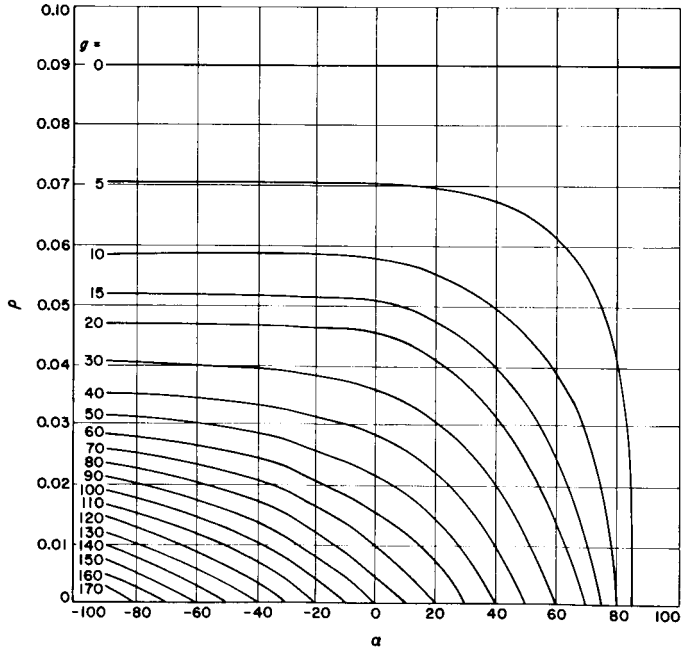

Fig. 4. Lunar reflectance function; Sytinskaya data

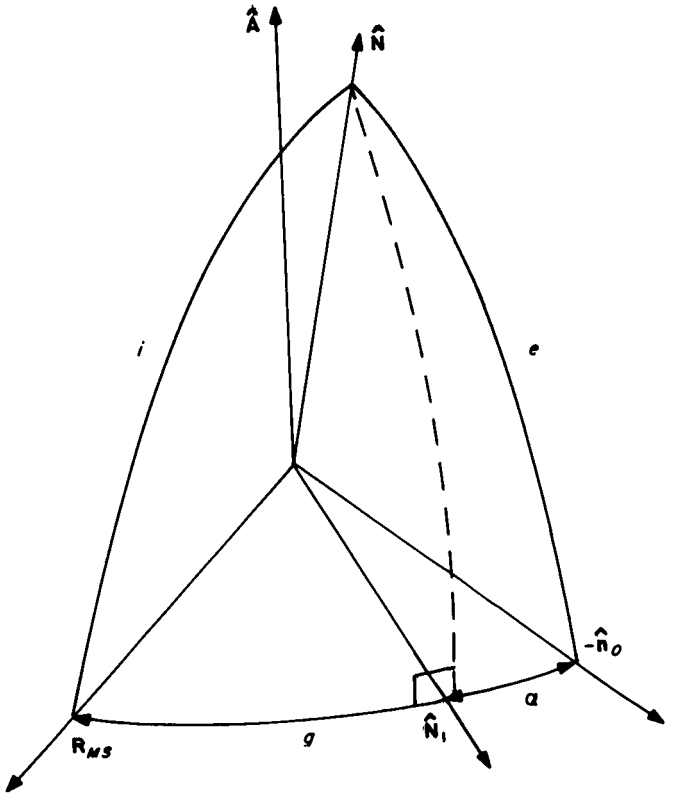

Fig. 5. Angle α in terms of spacecraft geometry

where the vector identities for arbitrary vectors **A**, **B**, **C**, and **D**

$$\mathbf{A} \times (\mathbf{B} \times \mathbf{C}) = \mathbf{B}(\mathbf{A} \cdot \mathbf{C}) - \mathbf{C}(\mathbf{A} \cdot \mathbf{B})$$

and

$$(\mathbf{A} \times \mathbf{B}) \cdot (\mathbf{C} \times \mathbf{D}) = \mathbf{C} \cdot [\mathbf{D} \times (\mathbf{A} \times \mathbf{B})]$$

have been used. Then, using Eq. (2), the expression for α can be written as

$$\sin \alpha = \frac{\cos g \cos e - \cos i}{[\cos^2 i + \cos^2 e - 2 \cos i \cos e \cos g]^{1/2}} \tag{3}$$

where it is assumed that $0 \leq i < \pi/2$, $0 \leq e < \pi/2$, and $0 < g < \pi$.

This, then, specifies the lunar reflectance properties to be used under the first approximation of Earth-based observations and homogeneity and relates them to the viewing geometry discussed earlier. Contrasts due to local surface orientations about a feature can now be obtained by calculating g and α for each normal **N** and finding ρ from the relation $\rho = \rho(g, \alpha)$.

C. Television and Recording System

The function of the system to be considered here consists of imaging a luminance distribution on a vidicon face, processing the resulting electrical signals through the electronics, reconstructing them on a kinescope, and forming a photographic positive of the kinescope reproduction of the scene. The input and output functions, respectively, are taken to be the luminance distribution being viewed and the transmission distribution on the output film positive. (The output could just as well have been taken to be a luminance distribution, but this differs only by a multiplicative constant from the transmission distribution, and the constant depends on the source illuminating the transparency.)

First to be determined is the transfer function for the system, that is, the output transmission as a function of the luminance of a uniform input scene. For fixed system parameters, the output transmission is solely dependent on the time-integrated spectral irradiance (energy per area per wavelength) of the vidicon's photoconductive surface weighted with the vidicon's spectral response function. From experimental evidence, it is apparently reasonable to assume that vidicons have intensity-independent spectral response or photon efficiency functions. Thus, if $H(\lambda)$ is the spectral irradiance of a photoconductive surface (power per area per wavelength) and $f_V(\lambda)$ is the vidicon's spectral response function, the time-integrated "vidicon illuminance" (vidicon luminous flux per area)* dQ_V/dA' on which the output transmission depends is given by

$$\frac{dQ_V}{dA'} = \int_0^{\delta\tau} d\tau \int_0^{\infty} d\lambda H(\lambda) f_V(\lambda) \tag{4}$$

where $\delta\tau$ is the exposure time. Thus, once the output transmission as a function of the time-integrated vidicon illuminance of the photoconductive surface is

*"Vidicon luminous flux" is defined as the analog of standard visual luminous flux but with the vidicon's spectral-sensitivity curve instead of that of the human eye.

known, the system response to a uniform input with any spectral distribution $H(\lambda)$ can be predicted.

It is useful to calculate dQ_V/dA' in terms of the luminance of the object being viewed in photovisual units, since all the available lunar photometric data are in these units. Let a small plane area element δA be located in the camera's field of view very distant from the lens compared to its focal length F, and let $\mathbf{r}_c$ be the position vector of the center of δA in a camera-lens-centered coordinate system, where the lens lies in the uv-plane (Fig. 6). Let the area δA have a unit normal $\hat{\mathbf{N}}$ and spectral radiance $N(\lambda, \hat{\mathbf{e}})$ (power radiated per wavelength per solid angle per emitter area projected normal to the emission direction $\hat{\mathbf{e}}$). In the present case, $\hat{\mathbf{e}} = -\mathbf{r}_c/|\mathbf{r}_c| = -\hat{\mathbf{r}}_c$. Then, letting the lens have an area $A_{\mathcal{L}}$, the spectral radiant flux $\delta P(\lambda)$ incident on the lens from δA is approximately

$$\delta P(\lambda) \approx \frac{A_{\mathcal{L}} |\hat{\mathbf{r}}_c \cdot \hat{\mathbf{n}}_a|}{|\mathbf{r}_c|^2} \times \delta A \, |\hat{\mathbf{r}}_c \cdot \hat{\mathbf{N}}| \, N(\lambda, -\hat{\mathbf{r}}_c)$$

If the lens has a spectral radiant transmittance $t_{\mathcal{L}}(\lambda)$ and using Eq. (A-11) from Appendix A to find the image area $\delta A'$ of the object δA (assuming perfect focus), the time-integrated vidicon illuminance dQ_V/dA' incident on the vidicon's photoconductive surface (see Eq. 4) is

$$\begin{aligned}\frac{dQ_V}{dA'} &= \lim_{\delta A \to 0} \int_0^{\delta\tau} d\tau \int_0^{\infty} d\lambda \frac{\delta P(\lambda)}{\delta A'} t_{\mathcal{L}}(\lambda) f_V(\lambda) \\ &= \frac{A_{\mathcal{L}} |\hat{\mathbf{r}}_c \cdot \hat{\mathbf{n}}_a|^4}{F^2} \int_0^{\delta\tau} d\tau \int_0^{\infty} d\lambda \, N(\lambda, -\hat{\mathbf{r}}_c) \, t_{\mathcal{L}}(\lambda) f_V(\lambda)\end{aligned}$$

Assuming a constant emission rate, this can be rewritten as

$$\frac{dQ_V}{dA'} = \frac{\pi |\hat{\mathbf{r}}_c \cdot \hat{\mathbf{n}}_a|^4 \delta\tau}{4f^2} b_V(-\mathbf{r}_c) t_{\mathcal{L}} \tag{5}$$

where f is the lens f-number, $\delta\tau$ is the exposure time, $b_V(-\hat{\mathbf{r}}_c)$ is the vidicon luminance of the object surface, and $t_{\mathcal{L}}$ is the gross transmission coefficient of the lens, so that

$$b_V(-\hat{\mathbf{r}}_c) t_{\mathcal{L}} = t_{\mathcal{L}} \int_0^{\infty} d\lambda N(\lambda, -\hat{\mathbf{r}}_c) f_V(\lambda) = \int_0^{\infty} d\lambda N(\lambda, -\hat{\mathbf{r}}_c) t_{\mathcal{L}}(\lambda) f_V(\lambda)$$

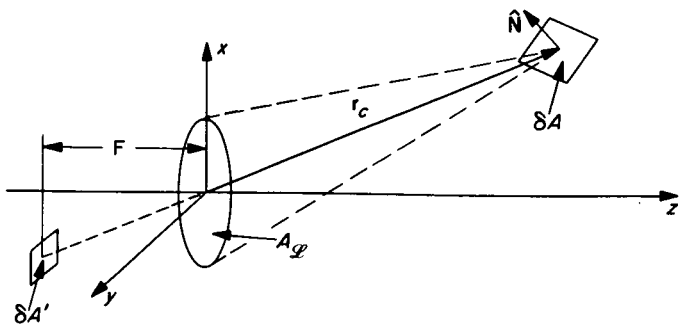

Fig. 6. Geometry for transfer-function calibration

Note that from Eq. (5), the vidicon luminous flux incident on the photoconductive surface is directly proportional to the object's luminance with respect to the vidicon's spectral-sensitivity curve. In fact, the vidicon luminous flux is proportional to the object's luminance with respect to any spectral-sensitivity curve including that of the human eye, but the proportionality constant depends on the spectral distribution of the source. That is, using the above notation, one has

$$b_V(-\hat{\mathbf{r}}_c) = \int_0^\infty d\lambda N(\lambda, -\hat{\mathbf{r}}_c) f_V(\lambda) = C_N \int_0^\infty d\lambda N(\lambda, -\hat{\mathbf{r}}_c) f_e(\lambda) = C_N b(-\hat{\mathbf{r}}_c)$$

where $f_e(\lambda)$ is the spectral sensitivity of the standard human observer and $b(-\mathbf{r}_c)$ is the photovisual luminance of the source. Obviously, the constant C_N depends upon the spectral distribution $N(\lambda, \hat{\mathbf{e}})$ of the source and the vidicon spectral response function $f_V(\lambda)$.

With these results in mind, then, the transfer function is just as meaningful in terms of the visual luminance of distant objects as it is in terms of the quantity dQ_V/dA' defined in Eq. (4) if care is taken with the spectral distribution of the source. Such a procedure was followed in the calibration of the *Ranger* cameras since, as mentioned earlier, all of the photometric information about the Moon is in photovisual units. Thus, the output film transmission t was determined as a function of the visual luminance b of a uniform object source with the same spectral distribution as that observed for light reflected from the lunar surface. Graphs of typical transfer functions will be found in Figs. 7 and 8.

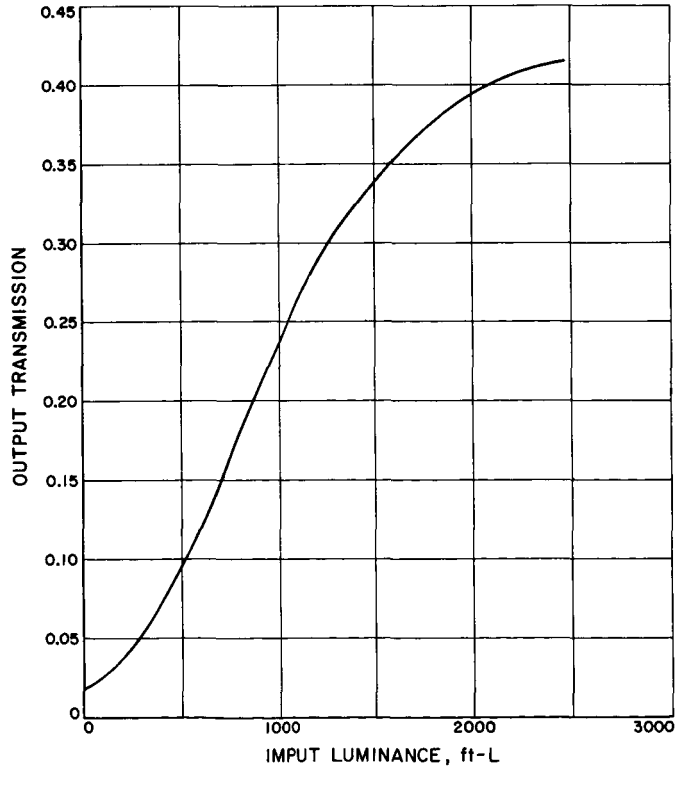

Fig. 7. Uniform source transfer function for *Ranger IX* P_1- and P_2-cameras

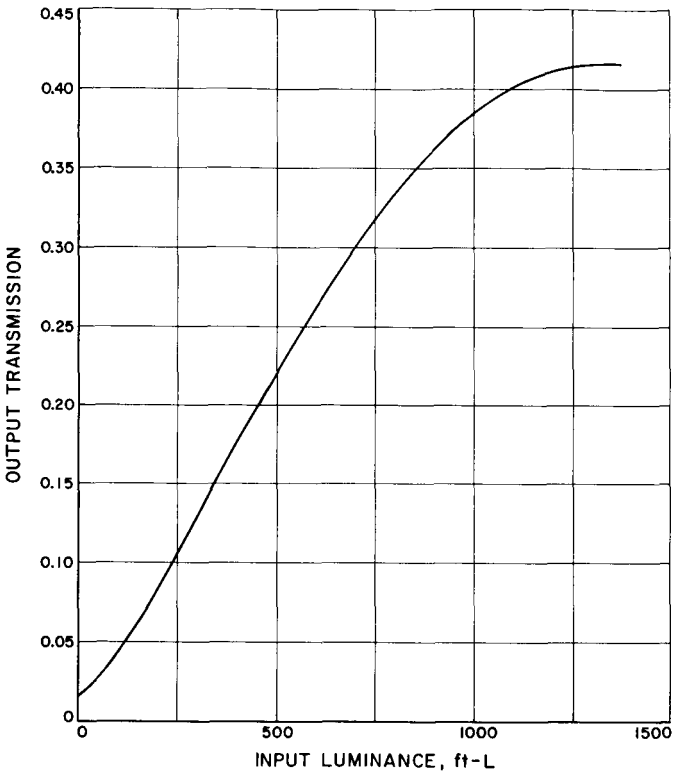

Fig. 8. Uniform source transfer function for *Ranger IX* P_3- and P_4-cameras

Whereas such transfer characteristics give the system response to a uniform scene input, one is interested in determining the system response to spatially varying scenes. A mechanism that might be used to describe this case at least in some first approximation is a two-dimensional analog of the familiar linear system analysis so useful in describing electrical and mechanical systems. Unfortunately, the justification for using this method for a complex television and recording system is not at all as clear as in the latter two cases, where well defined equations of motion apply. A summary of linear system analysis can be found in Appendix B, where it is pointed out that there are two important aspects to consider. First, a linear system, by definition, has a response to a sum of inputs which equals the sum of its responses to each element of the input sum irrespective of the others. Second, a complete orthogonal set of "characteristic" functions is required which, if processed through the system, are altered only in normalization.

One hopes that the first condition is reasonably satisfied if the luminance variations found in the input scene stay within a linear region of the transfer curve. This is highly probable, since, by the nature of the lunar reflectance function, scenes of very high contrast (neglecting shadows) are not to be expected. An obvious first candidate as the set of characteristic functions for the second condition is a set of two-dimensional sine waves. Since no theory exists to evaluate their suitability, experimental verification must be performed. It has not yet been possible to do this in detail, so it will simply be assumed that little harmonic distortion occurs for the system operating on a small-amplitude sine wave such as occurs in the Fourier decomposition of a low-contrast scene. Thus, as a

reasonable first approximation, the present system from object-scene luminance distribution to output-film transmission distribution will be considered linear and will be discussed in terms of two-dimensional Fourier linear system analysis.

Although only the results will be used here, an outline of such a formalism can be found in Appendix B. The system's response to nonuniform luminance distributions is calibrated by its response to a set of two-dimensional sine waves. Hence, one is interested in the system's response, as a function of spatial frequency, to luminance distributions of the form $b(u,v) = b_0 + \exp[i(k_u u + k_v v)]$, where b_0 is a constant greater than 1 (negative luminances are meaningless) and k_u and k_v are spatial frequencies in the (u,v) Cartesian coordinate system chosen as reference. The response of a linear system to such a stimulus, assuming a transfer function of the form $t = ab + t_0$, where a and t_0 are transfer constants and t and b are the output transmission and input luminance, respectively, is taken to be

$$t(\xi,\eta) = t_0 + a(u,v)\,b_0 + a(u,v)\,G(u,v,k_u,k_v)\exp[i(k_u u + k_v v)]$$

In this expression, $a(u,v)$ is a generalized transfer coefficient accounting for the scan-line structure and transfer nonuniformities in the output film, t_0 is the base film transmission, and $G(u,v,k_u,k_v)$ is the system *sine-wave response* or *modulation transfer* function accounting for changes in the phase and amplitude of the sine wave due to the dynamic response characteristics of the system. The coordinates (ξ,η) of the output are functions of the input coordinates (u,v) accounting for linear magnification, rotation, or geometric distortion. This result can be derived using scanning theory and by imposing further linearity conditions on parts making up the complex system, at least over the range of inputs for which the overall system response is taken to be linear.

For an arbitrary input luminance distribution $b(u,v)$ whose Fourier transform exists and is defined by

$$b(u,v) = \int_{-\infty}^{\infty} dk_u \int_{-\infty}^{\infty} dk_v B(k_u,k_v)\exp[i(k_u u + k_v v)]$$

and

$$B(k_u,k_v) = \frac{1}{(2\pi)^2}\int_{-\infty}^{\infty} du \int_{-\infty}^{\infty} dv\, b(u,v)\exp[-i(k_u u + k_v v)]$$

the expression for the output transmission distribution is

$$t(\xi,\eta) = t_0 + a(u,v)\int_{-\infty}^{\infty} dk_u \int_{-\infty}^{\infty} dk_v B(k_u,k_v)\,G(u,v,k_u k_v)\exp[i(k_u u + k_v v)] \tag{6}$$

This can be written in the form of a convolution integral like Eq. (B-5), so that

$$t(\xi,\eta) = t_0 + \frac{a(u,v)}{(2\pi)^2}\int_{-\infty}^{\infty} dr \int_{-\infty}^{\infty} ds\, b(u-r, v-s)\,g(u,v,r,s) \tag{7}$$

where

$$g(u,v,r,s) = \int_{-\infty}^{\infty} dk_r \int_{-\infty}^{\infty} dk_s G(u,v,k_r,k_s)\exp[i(k_r r + k_s s)]$$

The system transfer function having been determined earlier, the sine-wave response function remains to be found. It will be assumed to be uniform over the vidicon surface and, thus, a function of spatial frequency only. Since the

system sine-wave response function is in general complex, its determination requires the measurement of two independent quantities. These will be taken to be the amplitude and phase.

The amplitude portion is measured simply by placing illuminated photographic transparencies with spatially sinusoidal transmission distributions of different frequencies in the camera's field of view and determining the relative modulation changes in the output transparencies. Note that the *Ranger* system has fixed focus at infinity and fixed aperture, so that the detailed calibration is performed by placing the targets normal to the optical axis at infinity, say with a collimator. For a variable focus and/or aperture system, the calibration must be done as a function of focus and/or aperture, since these factors have effects on the system performance. In either case, the sine-wave response at a given spatial frequency must be determined as a function of the azimuthal orientation of the direction of the sine wave about the optical axis (let the "direction" be defined by a line in the plane of the transparency normal to the "ridges" of the sine wave). Because of the nature of the raster scanning process, certain symmetries can be imposed on the sine-wave response function with respect to its azimuthal variation. The raster forms a natural Cartesian coordinate set with one axis parallel and one axis normal to the scan lines. Let the coordinates in this system be (u, v) as described above. Then, if the scanning beam has a symmetrical current cross section about the longitudinal axis, the following symmetries can be imposed at least on the amplitude portion of the sine-wave response function. They are, using the notation introduced earlier,

$$G(u, v, k_u, k_v) = G(u, v, -k_u, k_v)$$

and

$$G(u, v, k_u, k_v) = G(u, v, k_u, -k_v)$$

These symmetries correspond to cases in which the sine-wave directions are oriented symmetrically about the axis parallel to and normal to the scan lines, respectively.

Experimental measurements show that the contours of constant sine-wave response are regular and convex for the systems examined. They will be assumed to be ellipses with major and minor axes along the principal Cartesian axes defined above. This orientation of the major and minor axes is dictated by the symmetry properties of the sine-wave response function. In this case, therefore, only the response characteristics parallel and normal to the scan lines need be determined. Representative curves for the *Ranger* cameras can be found in Figs. 9 through 12.

It is pointed out that these curves are approximated rather well for analytic purposes by Gaussian functions of the form

$$G(k_u, k_v) = \exp\left[-\frac{1}{2}\left(\frac{k_u^2}{\sigma_u^2} + \frac{k_v^2}{\sigma_v^2}\right)\right] \tag{8}$$

where the u- and v-axes will be chosen to be parallel and normal to the scan lines, respectively.

The phase-shift portion of the sine-wave response function is much more difficult to measure. The main reason for this is that the amplitude portion of the response function is quite small compared with the noise for frequencies at which the phase shift becomes significant compared to geometric distortion.

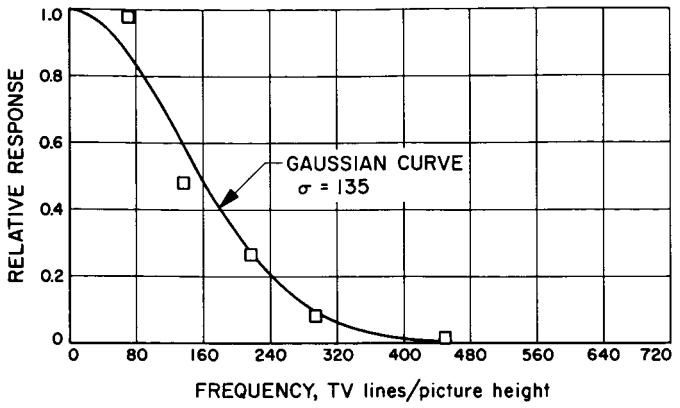

Fig. 9. *Ranger VII* full-scan camera sine-wave response (parallel to scan lines)

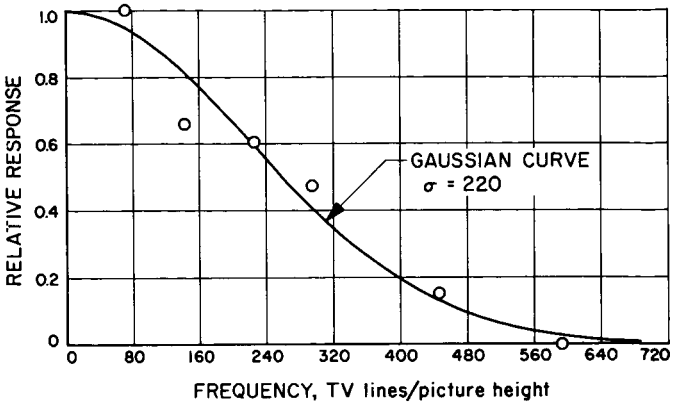

Fig. 10. *Ranger VII* full-scan camera sine-wave response (normal to scan lines)

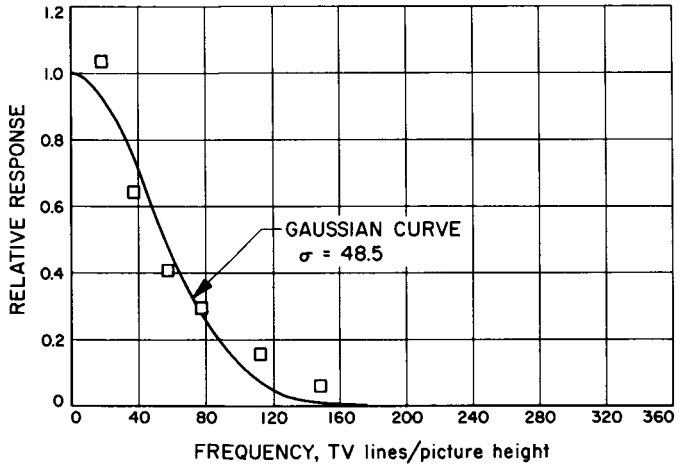

Fig. 11. *Ranger VII* partial-scan camera sine-wave response (parallel to scan lines)

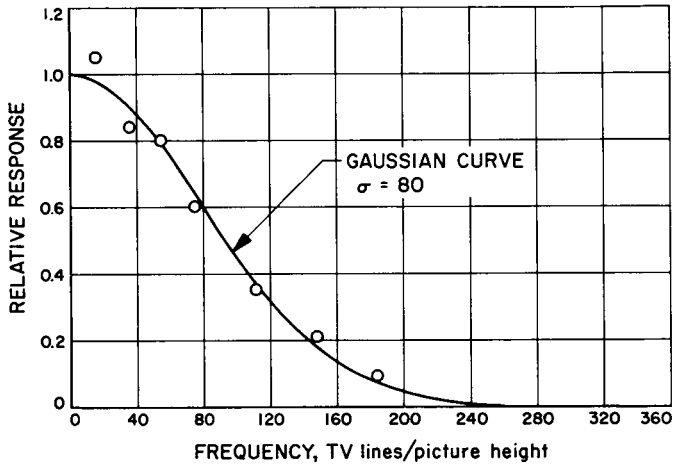

Fig. 12. *Ranger VII* partial-scan camera sine-wave response (normal to scan lines)

Thus, the phase portion of the sine-wave response function will be considered constant over the region where the amplitude part makes significant contributions. In this case, Eq. (8) gives the complete system sine-wave response function.

Thus, with the transfer function constants t_0 and a and the Gaussian widths σ_u and σ_v determined from system calibration data, Eq. (6) or (7) can be used to predict the system response $t(\xi, \eta)$ to any nonuniform object scene luminance $b(u, v)$. The truth of this statement is, of course, predicated on the accuracy with which linear system analysis can be applied to describe the system.

As the final part of the system description, there remains the inherent noise in the output film facsimile, which will tend to obscure detail in the reproduction. Virtually all components of the system contribute to the final noise level, as for example, the camera electronics, the telemetry process, the ground processing electronics, the output kinescope face, and the grain structure of the output transparency. A detailed study of the propagation of noise from the various components through the system to the output, taking into account the local statistics of noise generation and the transfer characteristics between various intermediate components all as a function of pertinent system parameters and environmental

conditions, would be somewhat formidable. Some measurements have in fact been performed on typical *Ranger* systems, with the result that the output electrical noise spectrum is found not to be simple but to exhibit rising and falling characteristics in various portions of the 200-kc overall system bandwidth. These complications are due to the spectral shaping characteristics of various system components needed to give a uniform spectral response over the 200-kc bandwidth to the input vidicon signals. Since the noise introduced at various points throughout the system can in general be considered "white," the output noise spectrum is other than white, having been distorted by the shaping spectra. In addition, the inclusion of telemetry noise (although a small factor here), with its triangular noise spectrum rising with frequency, further complicates the output electrical noise spectrum. It is noted that the noise spectrum is fairly flat at low frequencies (≤ 8 kc) and rises for higher frequencies out to 200 kc. The film recording process has a falling sine-wave response function essentially for all spatial frequencies. This falling characteristic will tend to offset the rising electrical noise characteristic and make the assumption of a white-noise spectrum more realistic. Furthermore, the grain noise in the film has a spectral distribution that generally falls with increasing spatial frequency, thereby again weighting the low-frequency end of the spectrum and offsetting the electrical spectrum. For these reasons (although no experimental verification has yet been performed), to obtain a good first approximation, and for mathematical simplicity, the noise spectrum in the output film will be taken as flat in spatial frequency and independent of direction. This excludes the scan-line structure, which is very directional and periodic but which must be considered as a type of noise if the pictures are greatly affected by its presence. For the *Ranger* system, however, there is considerable scan-line overlap, so that the effects of the scan lines are assumed to be negligible.

In the output transparency, the noise manifests itself as transmission fluctuations about some mean transmission value. The amplitude of these fluctuations certainly depends upon the mean transmission value, since neither a very dense nor a very transparent piece of film exhibits much noise, whereas intermediately exposed films have considerable noise levels. The amplitude of such noise can be measured with a scanning microphotometer as described below.

In Appendix C, the relationship between the rms noise of interest here and the output of a microphotometer is discussed in detail. Only the results specialized to the above assumptions will be quoted. Let $t(\xi, \eta)$ be the noisy reproduction of a spatially uniform input luminance distribution, so that

$$t(\xi, \eta) = t_1 + t_N(\xi, \eta) \tag{9}$$

where t_1 is the mean transmission and $t_N(\xi, \eta)$ is the white-noise term with zero average. If the assumed white-noise spectrum of amplitude $T_{N_0}(t_1)$ is spatially filtered by a device with a spectral response $F(k_\xi, k_\eta)$, $t_N(\xi, \eta, F)$, the filtered noise distribution, can be written in its Fourier representation using Eq. (C-2), as

$$t_N(\xi, \eta, F) = T_{N_0}(t_1) \int_{-\infty}^{\infty} dk_\xi \int_{-\infty}^{\infty} dk_\eta F(k_\xi, k_\eta) \exp\{i[k_\xi \xi + k_\eta \eta + \phi(k_\xi, k_\eta)]\}$$

where $\phi(k_\xi, k_\eta)$ is a real random variable for all k_ξ and k_η uniformly distributed over 2π. Then, if $\langle\ \rangle$ denotes a spatial average over the whole output distribution,

and if $\langle t_N(F)\rangle_{\text{rms}}$ is the average of the square of the noise fluctuations about the mean, it follows from Eq. (C-9) that

$$\langle t_N(F)\rangle^2_{\text{rms}} = \langle t^2(\xi,\eta,F)\rangle - \langle t(\xi,\eta,F)\rangle^2 = T^2_{N_0}(t_1)\int_{-\infty}^{\infty} dk_\xi \int_{-\infty}^{\infty} dk_\eta \,|F(k_\xi,k_\eta)|^2 \tag{10}$$

The white-noise spectrum amplitude, $T_{N_0}(t_1)$, is then determined with a microphotometer, as follows. For a square scanning aperture of dimension d, if $t^a(\tau)$ is the time-dependent output of the microphotometer scanning the white-noise distribution, Appendix C shows the rms noise fluctuation about the mean, $\langle t^a_N\rangle_{\text{rms}}$, to be given by ($\langle\ \rangle$ denote an average over time here)

$$\langle t^a_N\rangle^2_{\text{rms}} = \langle [t^a(\tau)]^2\rangle - \langle t^a(\tau)\rangle^2 = T^2_{N_0}(t_1)\left[\frac{2}{d}\right]^4 \int_{-\infty}^{\infty} dk_\xi \int_{-\infty}^{\infty} dk_\eta \frac{\sin^2\dfrac{k_\xi d}{2}}{k_\xi^2}\,\frac{\sin^2\dfrac{k_\eta d}{2}}{k_\eta^2}$$

Solving for $T^2_{N_0}(t_1)$,

$$T^2_{N_0}(t_1) = \frac{\langle t^a_N\rangle^2_{\text{rms}}\, d^2}{(2\pi)^2} \tag{11}$$

Finally, combining Eqs. (10) and (11), the rms film noise after arbitrary spatial filtering (ultimately by an observer) is shown to be

$$\langle t_N(F)\rangle^2_{\text{rms}} = \frac{\langle t^a_N\rangle^2_{\text{rms}}\, d^2}{(2\pi)^2}\int_{-\infty}^{\infty} dk_\xi \int_{-\infty}^{\infty} dk_\eta \,|F(k_\xi,k_\eta)|^2 \tag{12}$$

Thus, having determined the amplitude $T_{N_0}(t_1)$ of the white-noise spectrum, one can find, using Eq. (12), the rms noise level after any arbitrary filtering. The quantity $\langle t^a_N\rangle_{\text{rms}}\, d$, measured by the microphotometer, is plotted as a function of the mean transmission t_1 in Fig. 13 for a typical *Ranger* system.

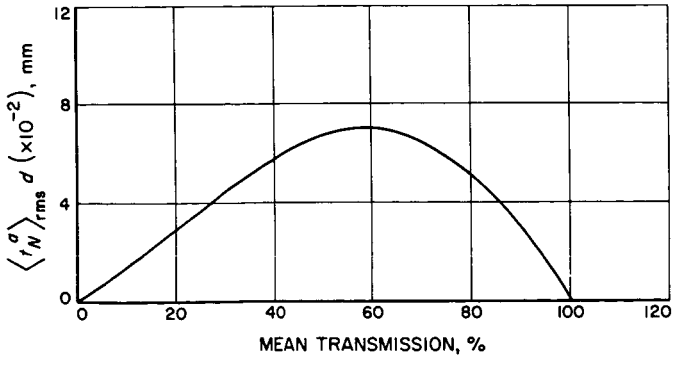

Fig. 13. Measured output film noise

The linear system analysis presented earlier, together with the above noise considerations, provides a unified and attractive description of the system. The justification for using linear system analysis and, in particular, for using sine waves as the characteristic functions of the system, rests entirely on "small signal" arguments. Whereas the rigor of such an approach may be questioned, it is felt that it offers at least a reasonable approximation to actual system performance.

D. Image Blur

Image blur has two basic origins within the system; namely, lack of focus, both electronic and optical, and relative motion between the camera and the object being viewed. For the present, perfect focus will be assumed throughout the system, so that only image motion need be considered. The effect of image motion on the detectability of a resolution element lies in the resulting contrast reduction. This can be simply described within the framework of linear system analysis as a modification to the system sine-wave response function, as follows.

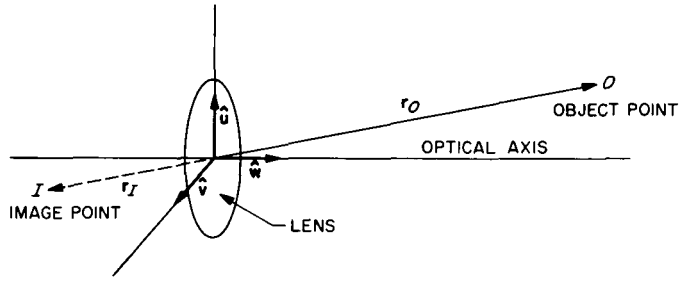

Fig. 14. Lens-centered coordinate system $(\hat{u}, \hat{v}, \hat{w})$

Let a *lens-centered coordinate system* be a right-handed Cartesian system with coordinates (u, v, w) having their origin at the center of the lens, which is taken to lie in the uv-plane (see Fig. 14). Further, let $\mathbf{r}_O$ be the position vector of a point O in the camera's field of view, and let $\mathbf{r}_I$ be the position vector of its image I. Note that a unit vector set $(\hat{\mathbf{u}}, \hat{\mathbf{v}}, \hat{\mathbf{w}}) = (\hat{\mathbf{u}}, \hat{\mathbf{v}}, \hat{\mathbf{n}}_a)$ will be taken along the principal Cartesian directions, where $\hat{\mathbf{n}}_a$ is the unit vector along the optical axis introduced earlier in the discussion of the Moon-centered coordinate system. If it is assumed that the object point O is at a great distance from the lens compared with its focal length F, that is, if $\mathbf{r}_O \cdot \hat{\mathbf{n}}_a >> \mathrm{F}$, then, from Eq. (A-1) in Appendix A, one has

$$\mathbf{r}_I = \frac{-\mathrm{F}}{\mathbf{r}_O \cdot \hat{\mathbf{n}}_a} \mathbf{r}_O$$

Upon straightforward differentiation with respect to time, the velocity $\boldsymbol{v}_I = d\mathbf{r}_I/d\tau$ of the image point I is written in terms of the relative velocity $\boldsymbol{v}_O = d\mathbf{r}_O/d\tau$ of the object point O with respect to the camera as

$$\boldsymbol{v}_I = \frac{\mathrm{F}}{\mathbf{r}_O \cdot \hat{\mathbf{n}}_a} \frac{\hat{\mathbf{n}}_a \times (\hat{\mathbf{r}}_O \times \boldsymbol{v}_O)}{\hat{\mathbf{r}}_O \cdot \hat{\mathbf{n}}_a} \tag{13}$$

where the vector identity $\mathbf{A} \times (\mathbf{B} \times \mathbf{C}) = \mathbf{B}(\mathbf{A} \cdot \mathbf{C}) - \mathbf{C}(\mathbf{A} \cdot \mathbf{B})$ has been used for arbitrary vectors **A**, **B**, and **C**.

From Eq. (13), it is noted that the image velocity $\boldsymbol{v}_I$ is not a constant over the image plane even for constant relative velocity $\boldsymbol{v}_O$. The vector changes not only in magnitude but also in direction over the image plane. Thus, strictly speaking, a sine wave cannot be imaged as a simple sine wave under these conditions. To see the actual result, consider the following calculation.

Let a sine-wave test target of spatial frequency $\mathbf{k}$ be placed normal to the optical axis $\hat{\mathbf{n}}_a$ of a camera system. Given a coordinate system in the plane of this target, let the luminance distribution $b(\mathbf{x})$ of the sine wave be

$$b(\mathbf{x}) = b_0 \exp[i(\mathbf{k}\cdot\mathbf{x} + \phi)]$$

where b_0 and ϕ are constants and $\mathbf{x}$ is a position vector in the plane. Now, the problem is to calculate the time-averaged flux density distribution at the image plane if the camera system is moving with velocity $\boldsymbol{v}_O$ with respect to the sine-wave target. From Eq. (5), the flux density at the image plane of the camera is proportional to the object luminance and is independent of the object distance. (It is assumed that the object is close enough to the optical axis to make the $\cos^4$ vignetting factor essentially constant.) Consider a point on the sine-wave target with position vector $\mathbf{r}_0$ in the camera lens-centered coordinate system and $\mathbf{x}_0$ in the target-plane coordinate system at time $\tau = 0$. At time τ, the position vectors $\mathbf{r}$ and $\mathbf{x}$, locating the point in the sine-wave target which is imaged at the same point in the image plane as that at $\tau = 0$, are given by (see Fig. 15)

$$\mathbf{r} = \left[1 - \frac{\boldsymbol{v}_O\cdot\hat{\mathbf{n}}_a}{\mathbf{r}_0\cdot\hat{\mathbf{n}}_a}\tau\right]\mathbf{r}_0$$

and

$$\begin{aligned}\mathbf{x} &= \mathbf{x}_0 - \mathbf{r}_0 + \boldsymbol{v}_O\tau + \mathbf{r}\\ &= \mathbf{x}_0 + \tau\frac{\hat{\mathbf{n}}_a\times(\boldsymbol{v}_O\times\hat{\mathbf{r}}_0)}{\hat{\mathbf{r}}_0\cdot\hat{\mathbf{n}}_a}\end{aligned} \tag{14}$$

Thus, the time-integrated flux density dQ_V/dA' at the image point of interest is given by

$$\frac{dQ}{dA'} = Cb_0\exp[i(\mathbf{k}\cdot\mathbf{x}_0 + \phi)]\int_{\tau_0}^{\tau_0+\delta\tau}\exp\left[i\,\mathbf{k}\cdot\frac{\hat{\mathbf{n}}_a\times(\boldsymbol{v}_O\times\hat{\mathbf{r}}_0)}{\hat{\mathbf{r}}_0\cdot\hat{\mathbf{n}}_a}\tau\right]d\tau$$

where the derivation leading to Eq. (5) has been used and C represents the constants in that equation. So, one has

$$\frac{dQ}{dA'} = Cb_0\exp[i(\mathbf{k}\cdot\mathbf{x}_0 + \phi)]\frac{2\hat{\mathbf{r}}_0\cdot\hat{\mathbf{n}}_a}{\mathbf{k}\cdot[\hat{\mathbf{n}}_a\times(\boldsymbol{v}_O\times\hat{\mathbf{r}}_0)]}\sin\frac{1}{2}\mathbf{k}\cdot\frac{\hat{\mathbf{n}}_a\times(\boldsymbol{v}_O\times\hat{\mathbf{r}}_0)}{\hat{\mathbf{r}}_0\cdot\hat{\mathbf{n}}_a}\delta\tau\exp\left[i\,\mathbf{k}\cdot\frac{\hat{\mathbf{n}}_a\times(\boldsymbol{v}_O\times\hat{\mathbf{r}}_0)}{\hat{\mathbf{r}}_0\cdot\hat{\mathbf{n}}_a}\left(\tau_0 + \frac{\delta\tau}{2}\right)\right] \tag{15}$$

Now, the effective spatial filter due to image motion, $G_m(\mathbf{r}, \mathbf{k})$, is defined such that

$$\frac{dQ}{dA'} = Cb_0\,\delta\tau\,G_m(\hat{\mathbf{r}}, \mathbf{k})\exp[i(\mathbf{k}\cdot\mathbf{x} + \phi)]$$

where the position vector $\mathbf{x}$ is evaluated from Eq. (14) at time $\tau = \tau_0$, the start of the shutter cycle. Substituting Eq. (14) in Eq. (15), one has for the motion filter

$$G_m(\hat{\mathbf{r}}_0, \mathbf{k}) = \frac{2\hat{\mathbf{r}}_0\cdot\hat{\mathbf{n}}_a}{\mathbf{k}\cdot[\hat{\mathbf{n}}_a\times(\boldsymbol{v}_O\times\hat{\mathbf{r}}_0)]\,\delta\tau}\sin\frac{1}{2}\mathbf{k}\cdot\frac{\hat{\mathbf{n}}_a\times(\boldsymbol{v}_O\times\hat{\mathbf{r}}_0)}{\hat{\mathbf{r}}_0\cdot\hat{\mathbf{n}}_a}\delta\tau\exp\left[i\frac{1}{2}\mathbf{k}\cdot\frac{\hat{\mathbf{n}}_a\times(\boldsymbol{v}_O\times\hat{\mathbf{r}}_0)}{\hat{\mathbf{r}}_0\cdot\hat{\mathbf{n}}_a}\delta\tau\right]$$

Applying Eq. (13) to the present geometry, the image velocity $\boldsymbol{v}_I$ at time τ becomes

$$\boldsymbol{v}_I = \frac{\mathrm{F}}{\mathbf{r}_0\cdot\hat{\mathbf{n}}_a - \boldsymbol{v}_O\cdot\hat{\mathbf{n}}_a\tau}\frac{\hat{\mathbf{n}}_a\times(\hat{\mathbf{r}}_0\times\boldsymbol{v}_O)}{\hat{\mathbf{r}}_0\cdot\hat{\mathbf{n}}_a}$$

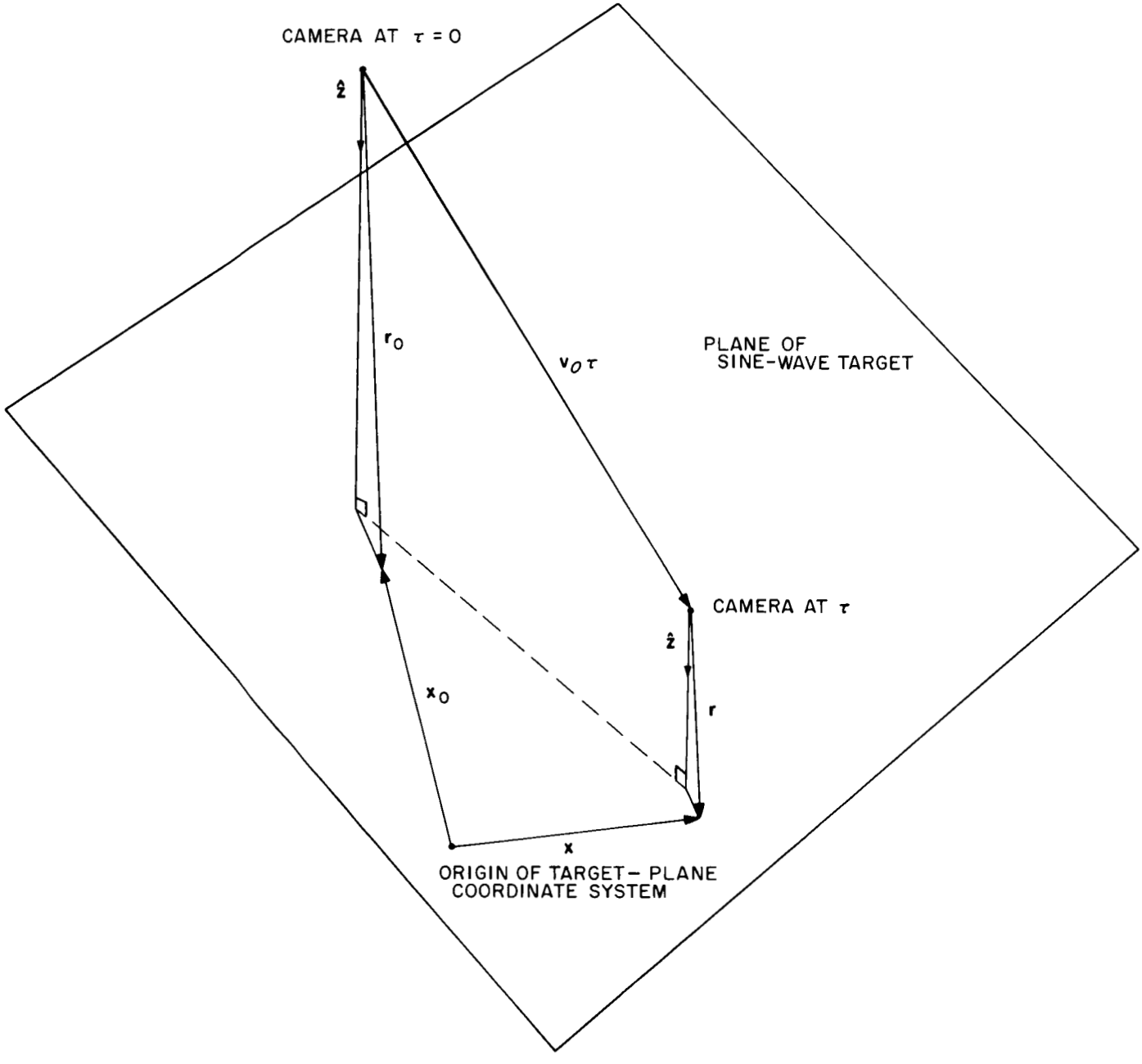

Fig. 15. Image motion geometry

Similarly, the spatial frequency $\mathbf{k}_I$ of the image sine wave at time τ is

$$\mathbf{k}_I = -\frac{\mathbf{r}_0 \cdot \hat{\mathbf{n}}_a - \boldsymbol{v}_O \cdot \hat{\mathbf{n}}_a \tau}{\mathrm{F}} \mathbf{k}$$

Finally, with

$$\mathbf{k}_I \cdot \boldsymbol{v}_I = \mathbf{k} \cdot \frac{\hat{\mathbf{n}}_a \times (\boldsymbol{v}_O \times \hat{\mathbf{r}}_0)}{\hat{\mathbf{r}}_0 \cdot \hat{\mathbf{n}}_a}$$

independent of time, the image motion filter becomes

$$G_m(\hat{\mathbf{r}}_0, \mathbf{k}_I) = \frac{2 \sin \frac{1}{2} \mathbf{k}_I \cdot \boldsymbol{v}_I \, \delta\tau}{\mathbf{k}_I \cdot \boldsymbol{v}_I \, \delta\tau} \exp\left(i \frac{1}{2} \mathbf{k}_I \cdot \boldsymbol{v}_I \, \delta\tau \right) \tag{16}$$

It is pointed out that G_m is not constant over the image plane even though the relative velocity vector $\boldsymbol{v}_0$ is. This arises from the form of Eq. (13), where it is evident that the image velocity $\boldsymbol{v}_I$ at any point in the image plane depends upon the direction of the position vector to that point. For the present purposes, however, since only small objects are of importance, it will be assumed that the points of interest in the image plane have position vectors with essentially the same direction. For these points, the velocity vector is almost constant, and Eq. (16) represents a well defined spatial filter. Note that this assumption is consistent with assuming a small enough field of view so that the $\cos^4$ vignetting factor in Eq. (5) is essentially constant. Thus, the image motion filter is well defined but is a function of the position of the small object of interest in the camera's field of view. In addition, the orientation of this velocity with respect to the television scan lines is a variable over the image plane, particularly if the relative velocity vector is contained in the field of view. This is quite likely for a nominal approach, since that configuration usually turns out to give the best resolution. Thus, the direction of the velocity $\boldsymbol{v}_I$ in Eq. (16) will be considered a random variable uniformly distributed over 360 deg. A meaningfully representative figure of merit is assumed to result from an average over the direction of the image velocity.

With the above assumptions, then, the effects of image motion on the threshold detectability of a resolution element can be included in a unified manner within the framework of linear system analysis.

E. Human Observer

Ultimately, the output facsimiles of the system must be presented to a human observer, who determines what information is in the picture. As mentioned earlier, the prime requisite for information perception is the detection of coherent detail in the system noise, which presumably requires some threshold signal-to-noise ratio. The detection process is most conveniently considered as a spatial filtering process. This, of course, assumes that the observer acts as a linear operator, but there is no real way to test whether he satisfies the necessary postulates (see Appendix C). Simply accepting this assumption, though, attempts have been made to measure the visual sine-wave response function under particular conditions, with the general result that an observer is found to act as a low-pass filter (Ref. 6). The detailed cutoff in absolute units of cycles per length must be a function of viewing geometry and the mental state of the observer. If he is allowed the freedom, an observer will alter the viewing conditions to optimize his visual output according to some criterion. This criterion must depend upon the task the observer is trying to perform, since the optimal configuration for correlation or interpreting detail over a large photograph would likely be different from that for detecting the smallest detail in a particular area. The effects of such optimization procedures are certainly significant in the interpretability of photographic information, so that an attempt to include them in a mathematical model must be made. Since the interest here lies in minimal detection capabilities of small detail in system noise,

it is reasonable to assume that the optimization criterion in this case is to maximize the signal-to-noise ratio of the visual output.

This observer function can be formulated mathematically as follows. Let the transmission distribution $t(\xi, \eta)$ presented to an observer have a spectral distribution $T(k_\xi, k_\eta)$ and let the superimposed transmission noise have a spectral distribution $T_N(k_\xi, k_\eta)$. Then, if the observer acts as a spatial filter with spectral distribution $G_O(k_\xi, k_\eta)$, his visual output-signal to rms-noise ratio, $S/N(\xi, \eta)$, is given by

$$\frac{S}{N}(\xi, \eta) = \frac{\int_{-\infty}^{\infty} dk_\xi \int_{-\infty}^{\infty} dk_\eta T(k_\xi, k_\eta)\, G_O(k_\xi, k_\eta) \exp[i(k_\xi \xi + k_\eta \eta)]}{\left\{\int_{-\infty}^{\infty} dk_\xi \int_{-\infty}^{\infty} dk_\eta |T_N(k_\xi, k_\eta)\, G_O(k_\xi, k_\eta)|^2\right\}^{1/2}} \tag{17}$$

(Note that the signals perceived by the observer are really in terms of luminances, but this represents only a multiplicative constant for both numerator and denominator in the S/N expression in terms of transmission and so divides out.) Here, of course, it is assumed that the observer acts as a linear operator. The signal-to-noise ratio in Eq. (17) has a maximum, $S/N|_0$, at some point (ξ_0, η_0). The observer then changes $G_O(k_\xi, k_\eta)$ until $S/N|_0$ is maximized.

Now, the question arises as to within what limits the observer can change his spatial filter characteristics. In this regard, two possibilities immediately come to mind. The first is that the functional form of $G_O(k_\xi, k_\eta)$ is altered to optimize $S/N|_0$. This case corresponds to the familiar "optimum filter" techniques of radar and communication theory, in which Schwarz's inequality is used to determine the functional form of $G_O(k_\xi, k_\eta)$ necessary to optimize $S/N|_{max}$. It turns out that

$$G_O(k_\xi, k_\eta) = C \frac{T^*(k_\xi, k_\eta)}{|T_N(k_\xi, k_\eta)|^2} \exp[-i(k_\xi \xi_0 + k_\eta \eta_0)] \tag{18}$$

where C is a real constant and it is assumed that $T_N(k_\xi, k_\eta)$ is nowhere zero. From Eq. (18) one notes that if the noise spectrum falls off fast enough for high frequencies, the observer filter must have a rising response characteristic. It would seem unreasonable to assign an observer such versatility.

A second and simpler, although less sophisticated, observer formulation is to let $G_O(k_\xi, k_\eta)$ be a low-pass filter such as a Gaussian, with a variable width parameter. In this case, the functional form of the filter stays fixed, but one or more parameters, such as the cutoff frequency, can be varied by such a simple maneuver as moving closer to or farther away from the picture. This formulation seems intuitively attractive and is consistent with measurements made to determine the sine-wave response function of the human observer. The optimization procedure for the observer is then to vary the allowed parameters until $S/N|_0$ is maximized. In this case, the observer filter $G_O(k_\xi, k_\eta)$ will be assumed in some first approximation to be a Gaussian with width parameter σ_0 and height G_{O_0}, so that

$$G_O(k_\xi, k_\eta) = G_{O_0} \exp\left[-\frac{1}{2\sigma_0^2}(k_\xi^2 + k_\eta^2)\right] \tag{19}$$

Then, if the noise spectrum $T_N(k_\xi, k_\eta)$ is assumed to be white with amplitude T_{N_0}, so that

$$T_N(k_\xi, k_\eta) = T_{N_0} \tag{20}$$

one has for Eq. (17)

$$\left.\frac{S}{N}\right|_0 = \frac{\int_{-\infty}^{\infty} dk_\xi \int_{-\infty}^{\infty} dk_\eta\, T(k_\xi, k_\eta) \exp\left[-\frac{1}{2\sigma_0^2}(k_\xi^2 + k_\eta^2)\right] \exp\left[i(k_\xi \xi_0 + k_\eta \eta_0)\right]}{\pi^{1/2} T_{N_0} \sigma_0} \tag{21}$$

Given $T(k_\xi, k_\eta)$ from the Fourier transform of Eq. (6), one calculates the numerator of Eq. (21) and maximizes the result with respect to σ_0. This is then the optimum signal-to-noise ratio $S/N|_{\max}$ as seen by the observer.

This $S/N|_{\max}$ represents the largest signal-to-noise ratio obtainable by the observer from looking at a resolution element and is used to determine the minimum detectable resolution-element size and, hence, the figure of merit. Note that again the effects of a system element, in this case the observer, are consistently included in the present scheme of analysis only to the extent that the element acts as a linear operator.

F. Summary

The results of the foregoing paragraphs constitute in some approximation a mathematical model of the complete system from input to observer, including all of the major degrading influences. All of these factors are included in a unified manner through linear system analysis and in particular through two-dimensional Fourier transform theory. In light of this, then, the major determining factor of the accuracy of the approximation is the degree of linearity of the system over the dynamic range under consideration. Since rather low-contrast object scenes are expected because of the lunar photometric properties, it is felt that at least local linearity of the transfer function over the luminance values found in such a scene is not an unreasonable assumption. Granted the linearity assumption, the model would seem to be a unified and accurate description of the effects of the various parts and aspects of the system upon its ultimate resolution capabilities. To be sure, a verification of the accuracy of the magnitudes of the numbers coming out of a calculation of the figure of merit requires extensive experimentation; such studies are underway. On the other hand, the relative magnitude of the figure of merit as a function of position on the lunar surface gives a reasonably meaningful measure of relative resolution and provides a useful criterion for choosing impact points for the *Ranger* vehicle, since it reaches a minimum value at some point.

IV. THE CALCULATION: PROCEDURE AND DETAILS

The application of the mathematical machinery described in Section III to the calculation of the figure of merit from its definition is straightforward even if somewhat involved. The general outline of the calculation appears below, followed by the mathematical details. The results from the preceding text and the Appendixes are freely drawn upon.

A. General Procedure

Assumed to be given are a specific orbital approach configuration as indicated in Fig. 1, the lunar reflectance characteristics as given in Fig. 4, and the television system characteristics. These latter characteristics include the system transfer and sine-wave response functions, the noise spectrum, and the geometrical parameters such as focal length, field of view, and output format size.

The first step in the calculation is to determine the contrasts between two resolution elements and the background surface, where one contrast is representative of areas brighter than the background and the other of areas darker than the background. Each is determined by averaging the surface-to-background luminance difference over the appropriate portion of the image of a cone and any shadow it throws. The surface of the cone is assumed to have the same photometric properties as the Moon, and the base angle of the cone is a constant for the calculation, nominally equal to 15 deg. The average is obtained for erect (apex up) as well as inverted (apex down) cones to include the effects of both depression- and protrusion-type features. The weighting function for the average is the size of an area element on the surface of the object cone after projection through the camera optics to the image plane of the vidicon.

Given these contrasts, the output transmission distribution for each resolution element is determined as a function of element size. This is accomplished by treating the system as linear and using Fourier analysis. Under this formalism, the degrading influences such as the television process, system optics, and image motion are treated in a unified manner as spatial filters.

Finally, knowing the output transmission distributions for both resolution elements, along with the output noise power spectrum, the maximum signal-to-rms noise ratio at a human observer's visual output is determined within the linear system scheme by assuming the observer to act as a variable-width low-pass spatial filter. This width is adjusted to optimize the output signal-to-noise ratio for each of the resolution elements. Then, using the condition for threshold detectability of the elements, one sets these optimum signal-to-noise ratios equal to 3, thereby determining the threshold-detectable resolution-element sizes, which are the only variables remaining in the problem. The reciprocal of the figure of merit is then taken to be the sum of the reciprocals of the cone diameters corresponding to the threshold resolution-element sizes.

B. Calculation Details

The contrast averaging for the resolution elements is done using the lunar reflectance function and the imaging and viewing geometry. The pertinent geometry is summarized below; the detailed derivations are omitted. Consider the case

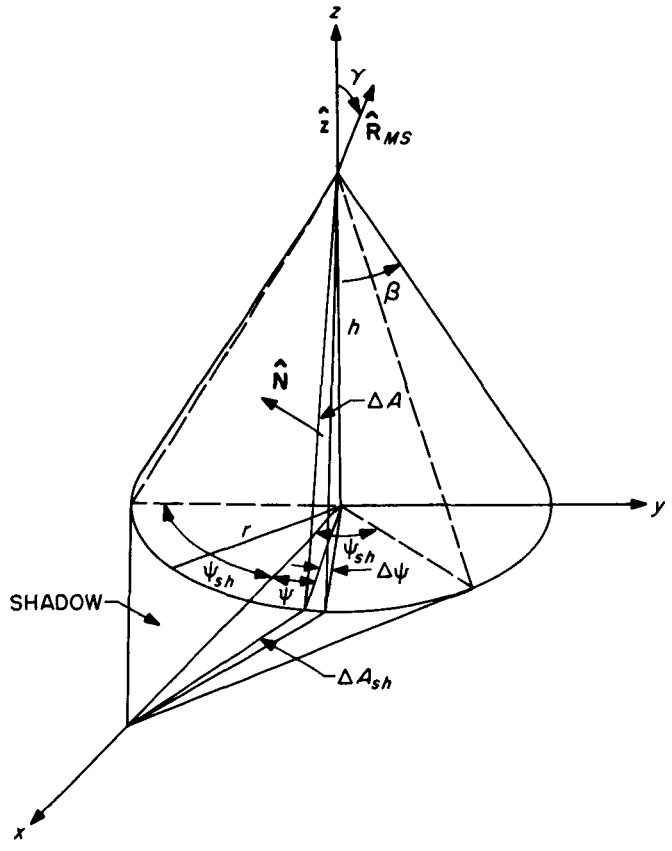

Fig. 16. Upright-cone geometry

of the upright cone first (see Fig. 16). Let the cone have a base of radius r and a height h, so that the half apex angle β is given by

$$\tan\beta = \frac{r}{h}, \qquad 0 < \beta < \frac{\pi}{2}$$

Let a Cartesian coordinate system be located such that the z'-axis is along the cone's axis, and the base is in the $x'y'$-plane. Let the x'-axis be in the plane determined by the z'-axis and the Moon–Sun direction $\hat{\mathbf{R}}_{MS}$, with the positive x'-axis opposite to the direction of the component of $\hat{\mathbf{R}}_{MS}$ in the $x'y'$-plane. Let $\hat{\mathbf{R}}_{MS}$ make an angle γ with the z'-axis, and let ψ be an azimuth angle in the $x'y'$-plane measured from the positive x'-axis. Now, for the contrast averaging, an area element ΔA about a generator of the cone and with normal $\hat{\mathbf{N}}$ can be written in terms of the azimuth-angle increment $\Delta\psi$ as

$$\Delta A = \frac{1}{2}\frac{r^2}{\sin\beta}\Delta\psi \tag{22}$$

The corresponding element ΔA_{sh} of the shadow area (assuming there is one) is

$$\Delta A_{sh} = \frac{1}{2}r^2\left(\frac{\tan\gamma}{\tan\beta}\cos\psi - 1\right)\Delta\psi \tag{23}$$

Note here that for a meaningful result, one must have

$$-\cos^{-1}\frac{\tan\beta}{\tan\gamma} < \psi < \cos^{-1}\frac{\tan\beta}{\tan\gamma}$$

which simply means that the shadow area ends for $\psi = \psi_{sh} = \pm\cos^{-1}(\tan\beta/\tan\gamma)$. Note further that ψ_{sh} has meaning only for $\gamma \geqq \beta$, which is the requirement for a shadow to exist at all. The above considerations assume that the observer can see all parts of the cone and shadow. That is, there is no "visual" shadow. This is generally the case with the *Ranger* impacting probe or the fly-by mission, but the more general projection case can be worked out with somewhat more complication.

So, given the normal $\hat{\mathbf{N}}$ to the area element ΔA (which is easily written as a function of the azimuth ψ), the illumination direction $\hat{\mathbf{R}}_{MS}$, and the observing camera look direction, the photometric geometry is easily worked out using Eqs. (2) and (3), so that the cone luminance is obtained from Fig. 4 as a function of ψ. The shadow luminance is zero (neglecting multiple reflections and Earth and star shine), and the background luminance is obtained similarly to that of the cone by noting that the background normal is simply $\hat{\mathbf{z}}'$ in this coordinate system. Thus, the average luminances about the upright cone above and below the background luminance are easily computed by choosing a suitably small $\Delta\psi$ and stepping ψ over 360 deg. The projected area elements are given by Eq. (A-11), where the necessary vectors are easily obtained from the viewing geometry.

The geometry and averaging are done similarly for the inverted cone, as summarized below. Let a coordinate system be defined for the inverted cone similar to that for the upright cone, as shown in Fig. 17. The only real difference, aside from the inversion of the cone, is the fact that the positive x'-axis is in the same direction as the component of $\hat{\mathbf{R}}_{MS}$ in the $x'y'$-plane. Again, there is a shadow produced if the colatitude γ of $\hat{\mathbf{R}}_{MS}$ is greater than the colatitude β of the generators of the cone. The endpoints of the shadow are given in terms of the azimuth ψ as

$$\psi = \psi_{sh} = \pm\cos^{-1}\frac{\tan\beta}{\tan\gamma}$$

Now, assuming that a shadow exists for

$$-\cos^{-1}\frac{\tan\beta}{\tan\gamma} < \psi < \cos^{-1}\frac{\tan\beta}{\tan\gamma}$$

the lateral area element ΔA_{sh} is all shadow, so that

$$\Delta A_{sh} = \frac{1}{2}\frac{r^2}{\sin\beta}\Delta\psi; \qquad -\cos^{-1}\frac{\tan\beta}{\tan\gamma} < \psi < \cos^{-1}\frac{\tan\beta}{\tan\gamma} \tag{24}$$

For ψ in the rest of the circle, the lateral area element is partly lit and partly shadow (assuming that there is a shadow). The shadow part, ΔA_{sh}, is given by

$$\Delta A_{sh} = \frac{1}{2}\frac{r^2}{\sin\beta}\left\{1 - \frac{4\left[2\sin^2\psi - \sin^2\psi_{sh}\left(1 + \dfrac{\cos\psi}{\cos\psi_{sh}}\right)\right][2\sin^2\psi + \tan^2\psi_{sh}(1 + \cos\psi\cos\psi_{sh})]}{(4\sin^2\psi + \sin^2\psi_{sh}\tan^2\psi_{sh})^2}\right\}\Delta\psi;$$

$$\cos^{-1}\frac{\tan\beta}{\tan\gamma} < \psi < 2\pi - \cos^{-1}\frac{\tan\beta}{\tan\gamma} \tag{25}$$

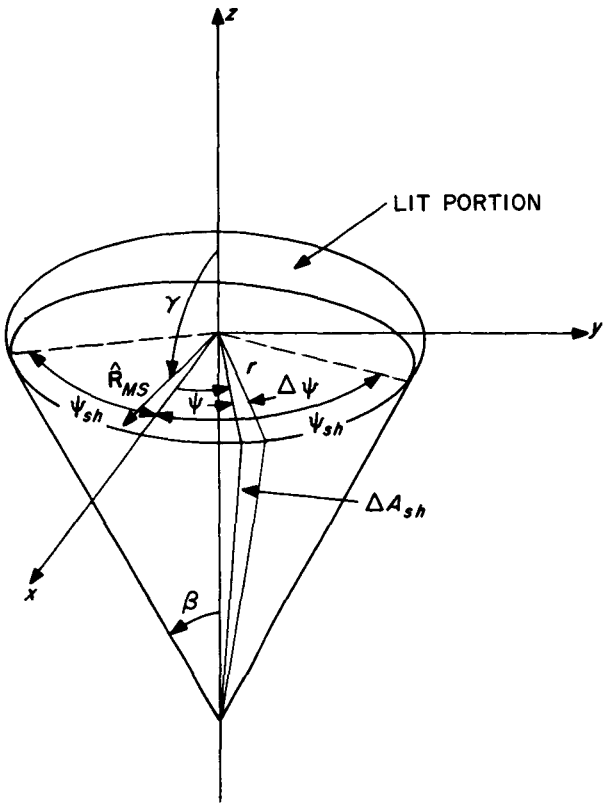

Fig. 17. Inverted-cone geometry

and the lit portion, ΔA, is given by

$$\Delta A = \frac{2r^2}{\sin\beta} \frac{\left[2\sin^2\psi - \sin^2\psi_{sh}\left(1 + \dfrac{\cos\psi}{\cos\psi_{sh}}\right)\right][2\sin^2\psi + \tan^2\psi_{sh}(1 + \cos\psi\cos\psi_{sh})]}{(4\sin^2\psi + \sin^2\psi_{sh}\tan^2\psi_{sh})^2}\Delta\psi;$$

$$\cos^{-1}\frac{\tan\beta}{\tan\gamma} < \psi < 2\pi - \cos^{-1}\frac{\tan\beta}{\tan\gamma} \tag{26}$$

Note that here again, it has been assumed that the whole interior of the inverted cone is visible to the observer, and the other case is similarly calculable. The averaging in this case is done just as before over those portions of the cone lighter and those darker than the background. Note also that all of the area elements in Eqs. (22) through (26) are proportional to the radius of the cone squared, making this factor unimportant in the averaging. Hence, the average contrasts depend only on the angular geometry, as must be the case, and not on the cone size.

Thus, given the light and dark contrast averages over the erect and inverted cones, the final contrasts to be used for the resolution elements are obtained by averaging the two light contrasts, using the total projected light areas for the two cases as weighting functions, and the dark areas for the dark contrasts.

The next step is to calculate the output transmission distributions for the two resolution elements as a function of size. Only the case of the light element is

considered, as that of the dark element is completely analogous. According to the earlier discussion of the television system, the form of the transfer function for a uniform input luminance is

$$t = t_0 + ab \tag{27}$$

where t is the output transmission, t_0 and a are transfer constants, and b is the uniform scene luminance. The assumption of transfer linearity is taken to be a good approximation for small changes in the luminance b, such as from the background luminance b_0 to the light resolution-element luminance b_L. The constant t_0 is unimportant here, since only output transmission differences are considered. The constant a is the transfer slope and is taken to be the average slope of the transfer curve (see Figs. 7 and 8) between the luminances b_0 and b_L. Then, from Eq. (6), and using the subsequent treatment of image motion, the transmission distribution $t(\xi, \eta)$ at the film output is

$$t(\xi, \eta) = t_0 + a \int_{-\infty}^{\infty} dk_u \int_{-\infty}^{\infty} dk_v\, B(k_u, k_v)\, G(k_u, k_v)\, G_m(k_u, k_v) \exp[i(k_u u + k_v v)] \tag{28}$$

where $B(k_u, k_v)$ is the Fourier transform of the input luminance distribution, $G(k_u, k_v)$ is the system sine-wave response (see Eq. 8), and $G_m(k_u, k_v)$ is the effective image-motion filter (see Eq. 16). It should be noted that the output coordinates (ξ, η) are functions of the vidicon coordinates (u, v). For the present purposes, distortion will be neglected, and it will be assumed that the relation involves only linear magnification by a factor μ, so that

$$(\xi, \eta) = (\mu u, \mu v) \tag{29}$$

In similar fashion, the output spatial frequencies (k_ξ, k_η) corresponding to (k_u, k_v) are given by

$$(k_\xi, k_\eta) = \left(\frac{k_u}{\mu}, \frac{k_v}{\mu}\right) \tag{30}$$

Equation (28) is written completely in terms of the output coordinates as

$$t(\xi, \eta) = t_0 + \mu^2 a \int_{-\infty}^{\infty} dk_\xi \int_{-\infty}^{\infty} dk_\eta\, B(\mu k_\xi, \mu k_\eta)\, G(\mu k_\xi, \mu k_\eta)\, G_m(\mu k_\xi, \mu k_\eta) \exp[i(k_\xi \xi + k_\eta \eta)] \tag{31}$$

This is the transmission distribution seen by the observer. (Note that actually the observer sees a luminance distribution, but this differs from the transmission distribution only by a constant. Since the signal-to-noise ratio is of importance here, and since the noise luminance and transmission distributions are related by the same constant, the constant divides out, and so luminance and transmission can be considered synonymous.) To include the effects of the observer on the output signal-to-noise ratio, one needs the Fourier transform $T(k_\xi, k_\eta)$ of the transmission distribution in Eq. (31). This transform is readily obtained as

$$T(k_\xi, k_\eta) = t_0\, \delta(k_\xi)\, \delta(k_\eta) + \mu^2 a\, B(\mu k_\xi, \mu k_\eta)\, G(\mu k_\xi, \mu k_\eta)\, G_m(\mu k_\xi, \mu k_\eta) \tag{32}$$

where $\delta(x)$ is the familiar Dirac delta function having the Fourier representation

$$\delta(x) = \frac{1}{2\pi} \int_{-\infty}^{\infty} dy \exp(ixy)$$

Consider now the input luminance distribution $b(u, v)$ due to a resolution element displayed against a uniform background and its Fourier transform $B(k_u, k_v)$. By definition, a resolution element is a square on the surface of the Moon in the camera's field of view, so that its shape on the vidicon face is the imaged projection of the square. For simplicity, the image will be assumed to be a rectangle whose sides are in the ratio of the minor and major axes of the image ellipse of a circle placed at the center of the field of view on the lunar surface. This ratio, κ, is obviously just the cosine of the angle between the optical axis and the surface normal. If $\mathbf{n}_a$ is a unit vector along the optical axis and $\hat{\mathbf{N}}$ is the unit surface normal, one has

$$\kappa = |\hat{\mathbf{n}}_a \cdot \hat{\mathbf{N}}| \tag{33}$$

Thus, the input luminance distribution $b(u, v)$ for the light resolution element as a function of its size l_l on the vidicon face is given by

$$b(u, v) = \begin{cases} b_L; & -\frac{l_l}{2} < u < \frac{l_l}{2} \text{ and } -\kappa\frac{l_l}{2} < v < \kappa\frac{l_l}{2} \\ b_0; & \text{otherwise} \end{cases} \tag{34}$$

Note here that an orientation with sides parallel and normal to the scan lines, respectively, has been chosen for simplicity. The Fourier transform, $B(k_u, k_v)$, of this distribution is calculated as

$$B(k_u, k_v) = \frac{1}{(2\pi)^2}\int_{-\infty}^{\infty} du \int_{-\infty}^{\infty} dv\, b(u, v)\, \exp[-i(k_u u + k_v v)]$$

or

$$B(k_u, k_v) = b_0\, \delta(k_u)\, \delta(k_v) + \frac{(b_L - b_0)}{\pi^2}\frac{\sin\frac{1}{2}k_u l_l}{k_u}\frac{\sin\frac{1}{2}k_v \kappa l_l}{k_v} \tag{35}$$

In calculating the output signal-to-noise ratio, one wants to consider only transmission changes above a constant background. The delta function terms in both Eq. (32) and Eq. (35) give rise to constant background terms and so will be neglected. Thus, the signal portion $B_S(k_u, k_v)$ is given by

$$B_S(k_u, k_v) = \frac{b_L - b_0}{\pi^2}\frac{\sin\frac{1}{2}k_u l_l}{k_u}\frac{\sin\frac{1}{2}k_v \kappa l_l}{k_v}$$

or

$$B_S(k_u, k_v) = \frac{(b_L - b_0)}{(2\pi)^2}\int_{-l_l/2}^{l_l/2} du \int_{-\kappa l_l/2}^{\kappa l_l/2} dv \exp[-i(k_u u + k_v v)] \tag{36}$$

From Eq. (8), the sine-wave response function $G(k_u, k_v)$ is given by

$$G(k_u, k_v) = \exp\left[-\frac{1}{2}\left(\frac{k_u^2}{\sigma_u^2} + \frac{k_v^2}{\sigma_v^2}\right)\right]$$

and from Eq. (16), the image-motion filter $G_m(k_u, k_v)$ is given by

$$G_m(k_u, k_v) = \frac{2 \sin \frac{1}{2} \mathbf{k}_I \cdot \boldsymbol{v}_I \, \delta\tau}{\mathbf{k}_I \cdot \boldsymbol{v}_I \, \delta\tau} \exp\left(\frac{1}{2} i \, \mathbf{k}_I \cdot \boldsymbol{v}_I \, \delta\tau\right)$$

or

$$G_m(k_u, k_v) = \frac{1}{\delta\tau} \int_0^{\delta\tau} dt \exp(i \, \mathbf{k}_I \cdot \boldsymbol{v}_I \, t) \tag{37}$$

Thus, the signal portion of the output-film transmission distribution, $T_S(k_\xi, k_\eta)$, is given by

$$T_S(k_\xi, k_\eta) = \frac{a(b_L - b_0)}{(2\pi)^2 \, \delta\tau} \int_0^{\delta\tau} dt \int_{-l/2}^{l/2} dx \int_{-\kappa l/2}^{\kappa l/2} dy \exp\left[-\frac{1}{2}\left(\frac{k_\xi^2}{\sigma_\xi^2} + \frac{k_\eta^2}{\sigma_\eta^2}\right)\right] \exp\{i[k_\xi(v_\xi t - x) + k_\eta(v_\eta t - y)]\} \tag{38}$$

where $\sigma_\xi = \sigma_u/\mu$, $\sigma_\eta = \sigma_v/\mu$, $l = \mu l_I$, $v_\xi = \mu v_u$, and $v_\eta = \mu v_v$. Then, including the effects of the observer as a low-pass filter $G_O(k_\xi, k_\eta)$, where it is assumed that

$$G_O(k_\xi, k_\eta) = G_{O_0} \exp\left[-\frac{1}{2\sigma_O^2}(k_\xi^2 + k_\eta^2)\right]$$

one has for the signal $S(\xi, \eta)$ at the observer's output (neglecting scale changes)

$$S(\xi, \eta) = \frac{a(b_L - b_0)}{(2\pi)^2 \, \delta\tau} G_{O_0} \int_0^{\delta\tau} dt \int_{-l/2}^{l/2} dx \int_{-\kappa l/2}^{\kappa l/2} dy \int_{-\infty}^{\infty} dk_\xi \int_{-\infty}^{\infty} dk_\eta \exp\left[-\frac{1}{2}\left(\frac{1}{\sigma_O^2} + \frac{1}{\sigma_\xi^2}\right) k_\xi^2 + i k_\xi (\xi + v_\xi t - x)\right]$$
$$\times \exp\left[-\frac{1}{2}\left(\frac{1}{\sigma_O^2} + \frac{1}{\sigma_\eta^2}\right) k_\eta^2 + i k_\eta (\eta + v_\eta t - y)\right] \tag{39}$$

Making the definitions

$$\frac{1}{\Sigma_\xi^2} = \frac{1}{\sigma_O^2} + \frac{1}{\sigma_\xi^2}$$

and

$$\frac{1}{\Sigma_\eta^2} = \frac{1}{\sigma_O^2} + \frac{1}{\sigma_\eta^2}$$

and performing the integrations over k_ξ and k_η, one has

$$S(\xi, \eta) = \frac{a(b_L - b_0)}{2\pi \, \delta\tau} \Sigma_\xi \Sigma_\eta G_{O_0} \int_0^{\delta\tau} dt \int_{-l/2}^{l/2} dx \int_{-\kappa l/2}^{\kappa l/2} dy \exp\left[-\frac{\Sigma_\xi^2}{2}(\xi + v_\xi t - x)^2\right] \exp\left[-\frac{\Sigma_\eta^2}{2}(\eta + v_\eta t - y)^2\right]$$

Then, using the definition of the error function

$$erfx = \frac{2}{\sqrt{\pi}} \int_0^x \exp(-u^2) \, du$$

and, making the substitution $t' = t - \delta\tau/2$, one has

$$S(\xi,\eta) = \frac{a(b_L - b_0)}{4\delta\tau} G_{o_0} \int_{-\delta\tau/2}^{\delta\tau/2} dt' \left[erf \frac{\Sigma_\xi}{\sqrt{2}} \left(\xi + v_\xi \frac{\delta\tau}{2} + v_\xi t' + \frac{l}{2} \right) - erf \frac{\Sigma_\xi}{\sqrt{2}} \left(\xi + v_\xi \frac{\delta\tau}{2} + v_\xi t' - \frac{l}{2} \right) \right]$$
$$\times \left[erf \frac{\Sigma_\eta}{\sqrt{2}} \left(\eta + v_\eta \frac{\delta\tau}{2} + v_\eta t' + \frac{\kappa l}{2} \right) - erf \frac{\Sigma_\eta}{\sqrt{2}} \left(\eta + v_\eta \frac{\delta\tau}{2} + v_\eta t' - \frac{\kappa l}{2} \right) \right]$$

It is easily shown that the maximum of this function occurs at the point

$$(\xi_0, \eta_0) = \left(-\frac{v_\xi \delta\tau}{2}, -\frac{v_\eta \delta\tau}{2} \right)$$

so that the spatially maximized signal S_0 is given by

$$S_0 = \frac{a(b_L - b_0)}{2\delta\tau} G_{o_0} \int_0^{\delta\tau/2} dt' \left[erf \frac{\Sigma_\xi}{\sqrt{2}} \left(v_\xi t' + \frac{l}{2} \right) - erf \frac{\Sigma_\xi}{\sqrt{2}} \left(v_\xi t' - \frac{l}{2} \right) \right] \left[erf \frac{\Sigma_\eta}{\sqrt{2}} \left(v_\eta t' + \frac{\kappa l}{2} \right) - erf \frac{\Sigma_\eta}{\sqrt{2}} \left(v_\eta t' - \frac{\kappa l}{2} \right) \right] \tag{40}$$

(Note also the symmetry of the integrand.) This integral cannot in general be written in closed form as is desirable for further manipulation. For the special case of one of the velocities being zero, it can be done, however. For example, letting $v_\eta = 0$ and $v_\xi = v$, one has

$$S_0 = \sqrt{\frac{2}{\pi}} \frac{a(b_L - b_0)}{\Sigma_\xi v \delta\tau} G_{o_0} \left\{ \sqrt{\frac{\pi}{2}} \frac{\Sigma_\xi}{2} \left[(v\delta\tau + l) erf \frac{\Sigma_\xi}{2\sqrt{2}} (v\delta\tau + l) - (v\delta\tau - l) erf \frac{\Sigma_\xi}{2\sqrt{2}} (v\delta\tau - l) \right] \right.$$
$$\left. + \exp\left[-\frac{\Sigma_\xi^2}{8} (v\delta\tau + l)^2 \right] - \exp\left[-\frac{\Sigma_\xi^2}{8} (v\delta\tau - l)^2 \right] \right\} erf \frac{\kappa \Sigma_\eta l}{2\sqrt{2}} \tag{41}$$

where the integral

$$\int erfx\,dx = x\,erfx + \frac{1}{\sqrt{\pi}} \exp(-x^2)$$

has been used. The case in which $v_\xi = 0$ and $v_\eta = v$ is easily written down by inspection. This assumption of having the image velocity in the cardinal Cartesian directions of the scanning raster is justified only by the ensuing simplicity, but it will be assumed that a representative resolution measure results from averaging the respective calculations for these two cases.

Then, assuming a white-noise spectrum for the system (the case of a shaped noise spectrum follows readily in principle from the foregoing formalism), the rms transmission noise $\langle t_N \rangle_{\text{rms}}$ at the observer's output is given by

$$\langle t_N \rangle_{\text{rms}} = \frac{(\langle t_N^a \rangle_{\text{rms}} d) G_{o_0} \sigma_o}{2\sqrt{\pi}} \tag{42}$$

where Eqs. (12) and (19) have been used. Note that the quantity $\langle t_N^a \rangle_{\text{rms}} d/2\pi$ is the noise power-spectrum amplitude as measured by a microphotometer and that expression (42) gives the rms noise amplitude after the white noise has been altered by the observer's effective spatial filter.

Thus, dividing Eq. (41) by Eq. (42), one obtains the spatially maximized signal-to-noise ratio $S/N|_0$ at the observer's output as

$$\left.\frac{S}{N}\right|_0 = \frac{2\sqrt{2}\,a\,(b_L - b_0)}{\sigma_\xi\,(\langle t_N^a\rangle_{\text{rms}}\,d)\,v\,\delta\tau}\,\frac{\sqrt{\sigma_0^2 + \sigma_\xi^2}}{\sigma_0^2}\left\{\sqrt{\frac{\pi}{2}}\,\frac{\Sigma_\xi}{2}\left[(v\,\delta\tau + l)\,erf\,\frac{\Sigma_\xi}{2\sqrt{2}}(v\,\delta\tau + l) - (v\,\delta\tau - l)\,erf\,\frac{\Sigma_\xi}{2\sqrt{2}}(v\,\delta\tau - l)\right]\right.$$
$$\left. + \exp\left[-\frac{\Sigma_\xi^2}{8}(v\,\delta\tau + l)^2\right] - \exp\left[-\frac{\Sigma_\xi^2}{8}(v\,\delta\tau - l)^2\right]\right\} erf\,\frac{\kappa\Sigma_\eta l}{2\sqrt{2}} \tag{43}$$

The symbols in Eq. (43) are summarized as follows:

a the transfer-function slope (see Eq. 27)

b_L the average luminance of the portion of the cone lighter than the background (this becomes b_D for the dark element)

b_0 the uniform background luminance

$\langle t_N^a\rangle_{\text{rms}} d/2\pi$ the noise power-spectrum amplitude as measured by a microphotometer with a square scanning aperture of dimension d (see Eq. 11)

v the image velocity on the output film (see Eq. 38)

$\delta\tau$ the exposure time

σ_ξ, σ_η the sine-wave response-function "widths" at the output film (see Eqs. 8 and 38)

σ_0 the observer spatial filter "width" at the output film (see Eq. 19)

$$\frac{1}{\Sigma_\xi^2}, \frac{1}{\Sigma_\eta^2} = \frac{1}{\sigma_\xi^2} + \frac{1}{\sigma_0^2}, \frac{1}{\sigma_\eta^2} + \frac{1}{\sigma_0^2}$$

κ the ratio between the sides of the image of the square resolution element (see Eq. 33)

$l, \kappa l$ the side lengths of the resolution-element image at the output film (see Eq. 38)

μ the magnification factor between the vidicon face and the output film (see Eq. 29)

To get the maximum signal-to-noise ratio $S/N|_{\max}$, Eq. (43) must be maximized with respect to the observer's spatial filter width σ_0. This optimum σ_0 is obviously going to be a function of the resolution-element dimension l. And since the minimum detectable l is obtained by requiring $S/N|_{\max}$ to be equal to 3, this dimension will also be a function of σ_0. So, the following set of simultaneous equations results:

$$\left.\frac{S}{N}\right|_0 = 3 \tag{44}$$

and

$$\left.\frac{\partial}{\partial\sigma_0}\frac{S}{N}\right|_0 = 0 \tag{45}$$

These expressions are straightforwardly evaluated using Eq. (43) to give

$$\frac{\sqrt{\sigma_0^2+\sigma_\xi^2}}{\sigma_0^2}\left\{\sqrt{\frac{\pi}{2}}\frac{\Sigma_\xi}{2}\left[(v\,\delta\tau+l)\,erf\frac{\Sigma_\xi}{2\sqrt{2}}(v\,\delta\tau+l)-(v\,\delta\tau-l)\,erf\frac{\Sigma_\xi}{2\sqrt{2}}(v\,\delta\tau-l)\right]+\exp\left[-\frac{\Sigma_\xi^2}{8}(v\,\delta\tau+l)^2\right]\right.$$
$$\left.-\exp\left[-\frac{\Sigma_\xi^2}{8}(v\,\delta\tau-l)^2\right]\right\}erf\frac{\kappa\Sigma_\eta l}{2\sqrt{2}}=\frac{3\,(\langle t_N^a\rangle_{rms}\,d)\,\sigma_\xi\,v\,\delta\tau}{2\sqrt{2}\,a\,(b_L-b_0)}$$

and

$$\sigma_0\frac{\sigma_0^2+\sigma_\xi^2}{(\sigma_0^2+2\sigma_\xi^2)}\left\{\sqrt{\frac{\pi}{2}}\frac{\sigma_\xi^3}{2\,(\sigma_0^2+\sigma_\xi^2)^{3/2}}\left[(v\,\delta\tau+l)\,erf\frac{\Sigma_\xi}{2\sqrt{2}}(v\,\delta\tau+l)-(v\,\delta\tau-l)\,erf\frac{\Sigma_\xi}{2\sqrt{2}}(v\,\delta\tau-l)\right]erf\frac{\kappa\Sigma_\eta l}{2\sqrt{2}}\right.$$
$$+\frac{\kappa l}{\sqrt{2\pi}}\frac{\sigma_\eta^3}{(\sigma_0^2+\sigma_\eta^2)^{3/2}}\left\{\sqrt{\frac{\pi}{2}}\frac{\Sigma_\xi}{2}\left[(v\,\delta\tau+l)\,erf\frac{\Sigma_\xi}{2\sqrt{2}}(v\,\delta\tau+l)-(v\,\delta\tau-l)\,erf\frac{\Sigma_\xi}{2\sqrt{2}}(v\,\delta\tau-l)\right]\right.$$
$$\left.\left.+\exp\left[-\frac{\Sigma_\xi^2}{8}(v\,\delta\tau+l)^2\right]-\exp\left[-\frac{\Sigma_\xi^2}{8}(v\,\delta\tau-l)^2\right]\right\}\exp\left(-\frac{\kappa^2\Sigma_\eta^2 l^2}{8}\right)\right\}$$
$$-\left\{\sqrt{\frac{\pi}{2}}\frac{\Sigma_\xi}{2}\left[(v\,\delta\tau+l)\,erf\frac{\Sigma_\xi}{2\sqrt{2}}(v\,\delta\tau+l)-(v\,\delta\tau-l)\,erf\frac{\Sigma_\xi}{2\sqrt{2}}(v\,\delta\tau-l)\right]\right.$$
$$\left.+\exp\left[-\frac{\Sigma_\xi^2}{8}(v\,\delta\tau+l)^2\right]-\exp\left[-\frac{\Sigma_\xi^2}{8}(v\,\delta\tau-l)^2\right]\right\}erf\frac{\kappa\Sigma_\eta l}{2\sqrt{2}}=0$$

The simplified case of no image motion ($v=0$) is somewhat simpler and can be shown to give

$$\frac{1}{\sigma_0}erf\frac{\Sigma_\xi l}{2\sqrt{2}}erf\frac{\kappa\Sigma_\eta l}{2\sqrt{2}}=\frac{3\,(\langle t_N^a\rangle_{\rm rms}\,d)}{2\sqrt{\pi}\,a\,(b_L-b_0)};\qquad v=0$$

and

$$\frac{\sigma_0 l}{\sqrt{2\pi}}\left[\frac{\sigma_\xi^3}{(\sigma_0^2+\sigma_\xi^2)^{3/2}}\exp\left(-\frac{\Sigma_\xi^2 l}{8}\right)erf\frac{\kappa\Sigma_\eta l}{2\sqrt{2}}+\frac{\kappa\sigma_\eta^3}{(\sigma_0^2+\sigma_\eta^2)^{3/2}}erf\frac{\Sigma_\xi l}{2\sqrt{2}}\exp\left(-\frac{\kappa^2\Sigma_\eta^2 l^2}{8}\right)\right]-\mathrm{erf}\frac{\Sigma_\xi l}{2\sqrt{2}}erf\frac{\kappa\Sigma_\eta l}{2\sqrt{2}}=0;\qquad v=0$$

as the set of simultaneous equations. The appropriate set is solved simultaneously to obtain σ_0 and l for the threshold-detectable resolution element. The element dimension l is the only quantity of importance for obtaining the figure of merit. Remembering, however, the special resolution-element orientation and image-velocity direction used in the preceding calculation, note that a truly representative element dimension should include an average over the other orientations. Such an average is justified for the velocity direction, since its direction changes over the image plane (see Eq. 13). For the other average, since the element is to be representative of images of actual features, the details of the feature outside of contrast are not of importance, so that such an average is desired. Then, because of the major simplifications resulting from choosing cardinal direction orientations for the image-velocity and element sides, a reasonable average will be assumed to result from averaging only over these two directions. Thus, letting v_ξ, v_η, l_ξ, and l_η represent the velocity and element side components in the cardinal directions, the average resolution-element dimension for threshold detection $l_{\rm av}$, is defined as

$$l_{\rm av}=\frac{1}{4}\left[l\,(v_\xi=v,v_\eta=0,l_\xi=l,l_\eta=\kappa l)+l\,(v_\xi=v,v_\eta=0,l_\xi=\kappa l,l_\eta=l)+l\,(v_\xi=0,v_\eta=v,l_\xi=l,l_\eta=\kappa l)\right.$$
$$\left.+\,l\,(v_\xi=0,v_\eta=v,l_\xi=\kappa l,l_\eta=l)\right]$$

The figure of merit is then determined simply by scaling the diameter of the object cone used for calculating the contrast averages, so that the average image area for conical depressions and protrusions lighter than the background has the same area as the average threshold-detectable resolution element κl_{tkv}^2. The diameter D_L thus obtained is the figure of merit for the lighter-than-background object.

A similar procedure is followed for the portion of the object cone which is darker than the background, so that one gets a diameter D_D for the threshold-detectable cone due to dark-area and shadow distributions. The final figure of merit is a combination of these, attempting to take into account the interaction between the light and dark portions. That is, a light and dark resolution-element pair is more easily detected than either an isolated light or dark element. On the other hand, if the threshold-detectable cone diameter due to lighter-than-background portions is much larger than that for dark portions, the threshold detection will take place primarily on the basis of dark portions. In the opposite

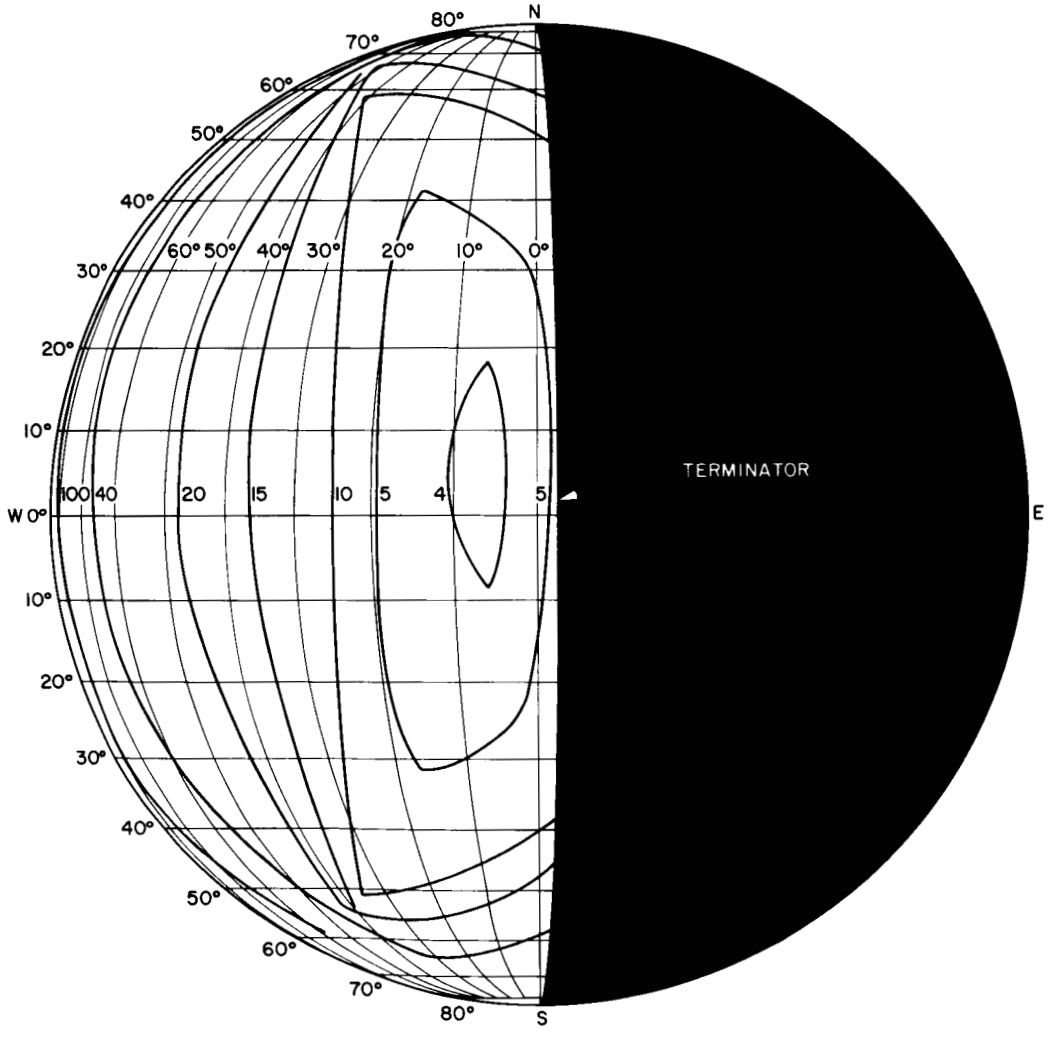

Fig. 18. *Ranger VII* preflight analysis, A-camera figure-of-merit contours

case, threshold detection will be based on the light portions. For these reasons, the final figure of merit or threshold-detectable cone diameter D (of given base angle) will be taken to be given by

$$\frac{1}{D} = \frac{1}{D_L} + \frac{1}{D_D} \tag{46}$$

where again D_L and D_D are the diameters of the threshold-detectable cones solely on the basis of lighter-than-background and darker-than-background areas.

Contours of constant figure of merit are shown as a function of impact point for two *Ranger* cameras and for a typical arrival geometry in Figs. 18 and 19. It will be noted that the figure of merit does indeed reach a minimum at some point on the lunar surface, indicating for the particular geometry and surface conditions assumed the optimum impact point from the point of view of best resolution.

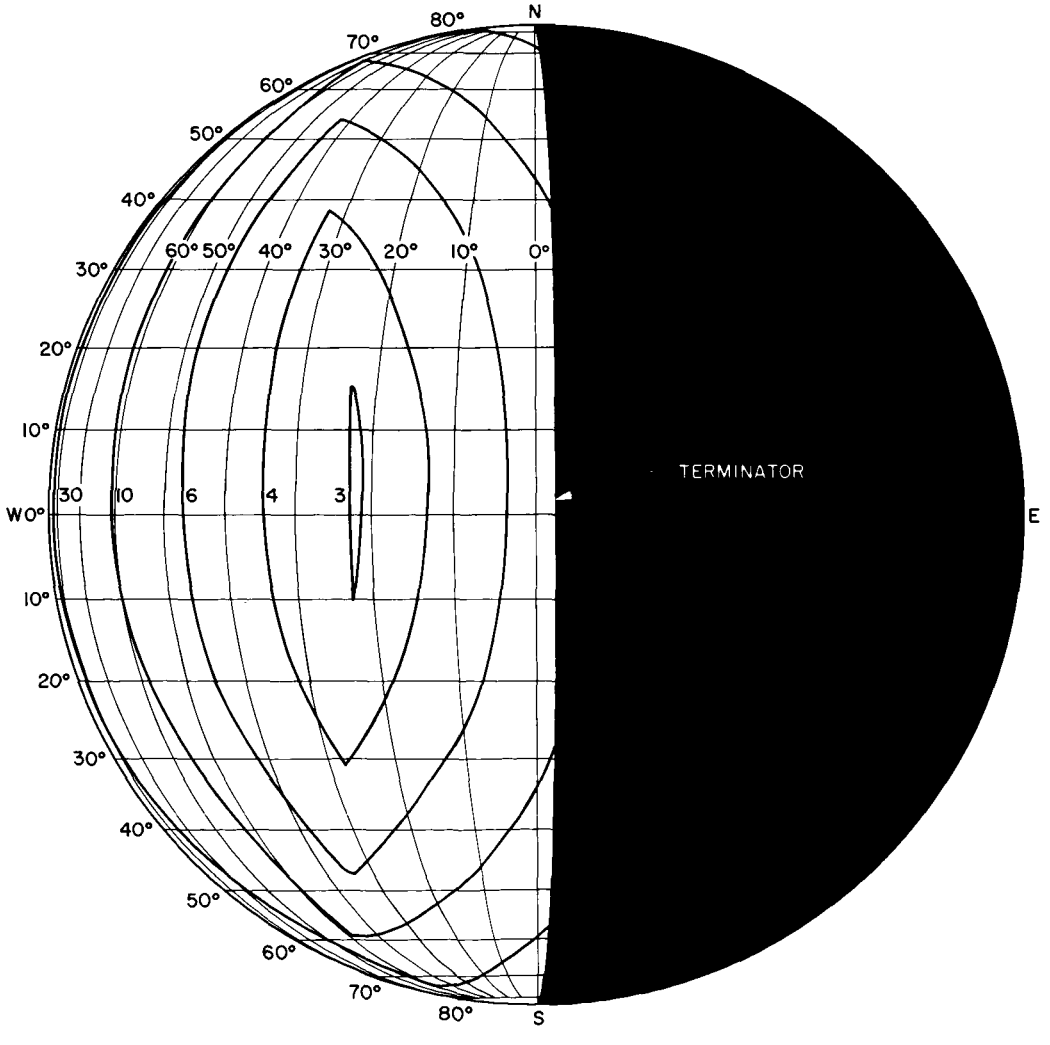

NOTE: NO TERMINAL MANEUVER,
30° BASE ANGLE FEATURE,
FRAME TIME 3.84 sec BEFORE
IMPACT, S/N RATIO=3.0

Fig. 19. *Ranger VII* preflight analysis, B-camera figure-of-merit contours

V. CONCLUSIONS: FIGURE OF MERIT VERSUS CONVENTIONAL RESOLUTION

The question naturally arises as to why one should use the present figure of merit rather than the more conventional measures of resolution. Normally, resolution for systems such as that aboard the *Ranger* is defined in terms of the ability of an observer to distinguish a series of light and dark bars after processing through the system involved. Usually, the object bars are of fixed contrast which is quite high. In light of earlier discussions, this method is seen to be closely related to simply determining, at one spatial frequency, the sine-wave response of the system, including the observer's filtering effects on the inherent noise and signal. To be sure, such an approach may be quite adequate if one is dealing with a scene of fixed contrast and viewing geometry having no image motion or other similar degrading effects. Such conditions obviously do not exist for lunar and planetary photographic missions. In particular, the Moon has somewhat unique photometric properties, and since object scene contrast is largely determined by the varying orientations of relief-feature surfaces, what can be seen in the system reproductions is intimately a function of the surface photometry and viewing geometry. Furthermore, since the system is carried on a spacecraft traveling at high velocity, the degradation due to image motion can be significant and also depends on the viewing geometry. Finally, the problem inherent in directing space probes is to choose a trajectory from which pictures with a maximum of information will be obtained. Conventional resolution criteria, which obviously do not account for the random physical properties of the scene, cannot give a rational approach to such problems nor even aid in their solution. Hence, the figure of merit.

This Report has discussed the application of a unified formalism to the solution of the above problems. Within the framework of linear system analysis, a reasonable approach for describing the effects of the expected low-contrast scenes, the viewing geometry, the surface photometry, the inherent facsimile system characteristics, the degrading influences such as image motion and system noise, and the capabilities of the human observer have been combined to give a single number or figure of merit characterizing the system resolution capabilities.

Even acknowledging the approximation inherent in the quantitative description of such a complicated system, it is felt that the figure of merit is a superior and far more versatile measure of system resolution capabilities than the conventional method, particularly in applications to complex random scenes. Obviously, if the effects of variable viewing geometry and photometry and image motion are removed, the figure of merit is comparable in meaning to the more conventional resolution definitions. Since this is not the case in space applications, the inclusion of these other effects is essential to a complete and unified description of the capabilities of a system. Thus, the figure of merit may be thought of as a unified generalization of conventional resolution-measuring criteria. The conventional approach has its place in engineering evaluations and comparison of various systems, but in applications to lunar and planetary photography, the figure of merit offers a more rational and complete resolution measure.

NOMENCLATURE

a	uniform field transfer-function slope
$\hat{\mathbf{A}}$	unit vector normal to plane containing incidence and emission directions
$A_{\mathscr{L}}$	area of lens
b_D	average luminance of portion of a cone darker than background
b_L	average luminance of portion of a cone lighter than background
b_V	vidicon luminance of object surface
$b(i, e, g)$	brightness of surface, ft-L
$b(u, v), b, b_0$	object scene luminance in photovisual unit system
$B(k_u, k_v)$	Fourier transform of $b(u, v)$
B_S, T_S	signal portion of luminance and transmission distributions
C_N	a constant
dQ_V/dA'	vidicon luminous flux per area
D	effective cone diameter of figure of merit value
D_L, D_D	minimum detectable cone diameters from light and dark criteria
e	reflected light-emission angle to camera
E_0	solar constant, ft-L
$f_e(\lambda)$	spectral sensitivity of standard human observer
$f_V(\lambda)$	vidicon spectral-response function
f	lens f-number
F	lens focal length
$F(k_\xi, k_\eta)$	spectral distribution of an arbitrary spatial filter
g	phase angle (angle between incidence direction and emission direction)
$G(u, v, k_u, k_v)$	system sine-wave response function at each point (u, v) in image plane
$G_m(\hat{\mathbf{r}}, \mathbf{k})$	effective spatial filter due to image motion
$G_0(k_\xi, k_\eta)$	observer spatial-filter spectrum
G_{0_0}, σ_0	parameters characterizing observer spatial filter
h	height of observed right-circular cone
$H(\lambda)$	spectral irradiance of a photoconductive surface
i	sunlight incidence angle
I	image of observed point

NOMENCLATURE (Cont'd)

(k_u, k_v), (k_ξ, k_η)	spatial frequency or wave-vector components in appropriate coordinate system
$\mathbf{k}_I$	spatial frequency or wave vector of sine wave in image plane
$l_I, \kappa l_I$	lengths of sides of resolution-element image on vidicon face
$\hat{\mathbf{n}}_a$	unit vector along spacecraft camera optical axis
$\hat{\mathbf{n}}_O$	unit vector from spacecraft camera to point O
$N(\lambda, \hat{\mathbf{e}})$	spectral radiance of δA in direction of emission $\hat{\mathbf{e}}$
$\hat{\mathbf{N}}$	unit vector normal to δA
$\hat{\mathbf{N}}_O$	unit vector normal to spherical lunar surface at point O
$\hat{\mathbf{N}}_1$	unit vector along component of $\hat{\mathbf{N}}$ in plane containing incidence and emission directions
O	observed point
r	radius of observed right-circular cone
$\mathbf{r}_c$	position of center of δA in camera lens-centered coordinate system
$\mathbf{r}_I$	position vector of image I of point O
$\mathbf{r}_O$	position vector of point O in camera field of view
$\hat{\mathbf{R}}_{MS}$	unit vector from Moon's center to Sun's center
$S/N(\xi, \eta)$	observer's visual output signal-to-rms noise ratio
$S/N\|_{\max}$	maximum value of $S/N\|_0$ with respect to σ_O
$S/N\|_0$	spatially maximized value of $S/N(\xi, \eta)$
$t(\xi, \eta), t, t_0$	output film transmission
$t^a(\tau)$	time-dependent output of microphotometer scan of a film transparency
$t_{\mathscr{L}}(\lambda)$	spectral radiant transmittance of lens
$t_N(\xi, \eta)$	film noise distribution
$\langle t_N \rangle_{\text{rms}}$	average of square of film transmission-noise fluctuation about the mean
$\langle t_N^a \rangle_{\text{rms}}$	average of square of microphotometer output fluctuations about the mean while scanning a film transparency with a square aperture of side d
t_1	mean transmission of film
$T(k_\xi, k_\eta)$	Fourier transform of $t(\xi, \eta)$
$T_N(k_\xi, k_\eta)$	transmission-noise spectral distribution
$T_{N_0}(t_1)$	white-noise spectrum amplitude
u, v	position coordinates in image plane of camera system

NOMENCLATURE (Cont'd)

$\boldsymbol{v}_I, \boldsymbol{v}_O$	velocity of image point and object point, respectively, in lens-centered coordinate system
$\boldsymbol{v}_{SC}$	velocity vector of spacecraft with respect to Moon-centered coordinate system
x, y, z	coordinate system in object space
α	luminance longitude
β	half apex angle of observed right-circular cone
γ	acute angle between $\hat{\mathbf{R}}_{MS}$ and axis of observed right-circular cone
δA	small plane area increment in object space
$\delta P(\lambda)$	spectral radiant flux incident on lens from δA
$\delta(x)$	Dirac delta function
$\delta\tau$	exposure time
ΔA	lateral area element of a cone
ΔA_{sh}	area element of shadow
κ	ratio between sides of image of a square resolution element
μ	linear magnification factor from image coordinate system to output coordinate system
ξ, η	position coordinates in output film
$\rho(i, e, g) = \rho(g, \alpha)$	lunar reflectance function
σ_u, σ_v	Gaussian width of camera sine-wave response
$\phi(k_\xi, k_\eta)$	a real random phase variable
ψ	azimuth angle in x, y cone base coordinate system
ψ_{sh}	azimuthal boundary of shadow area

REFERENCES

1. Schade, O. H., Sr., *An Evaluation of Photographic Image Quality*, Electron Tube Division, Radio Corporation of America, EM-7752, December 14, 1962, pp. 24–38.
2. Kopal, Z., Ed., *Physics and Astronomy of the Moon*, Academic Press, Inc., New York, 1961, p. 275.
3. Eimer, M., *Photography of the Moon from Space Probes*, Jet Propulsion Laboratory, California Institute of Technology, Technical Report No. 32-347, January 15, 1963.
4. Herriman, A. G., Washburn, H. W., and Willingham, D. E., *Ranger Preflight Science Analysis and the Lunar Photometric Model*, Jet Propulsion Laboratory, California Institute of Technology, Technical Report No. 32-384 (Rev.), March 11, 1963.
5. Willingham, D., *The Lunar Reflectivity Model for Ranger Block III Analysis*, Jet Propulsion Laboratory, California Institute of Technology, Technical Report No. 32-664, November 2, 1964.
6. Schade, O. H., Sr., "Electro-Optical Characteristics of Television Systems, Part 1," *RCA Review*, Vol. IX, March 1948, pp. 5–37.

APPENDIX A

Summary of Basic Imaging Geometry

In this Appendix, a review of the basic imaging geometry through simple, thin lenses is presented, along with brief derivations, for points, straight line segments, and plane areas. Expressions are specifically found for the case in which the object being imaged is at a great distance from the lens compared with the lens focal length.

Define a *lens-centered coordinate system* as a right-handed Cartesian system whose xy-plane coincides with the plane of a thin lens and whose origin is at the center of the lens (Fig. A-1). Let $\hat{\mathbf{x}}$, $\hat{\mathbf{y}}$, and $\hat{\mathbf{z}}$ be unit vectors along the principal Cartesian directions, and let object points for the lens have positive z-coordinates.

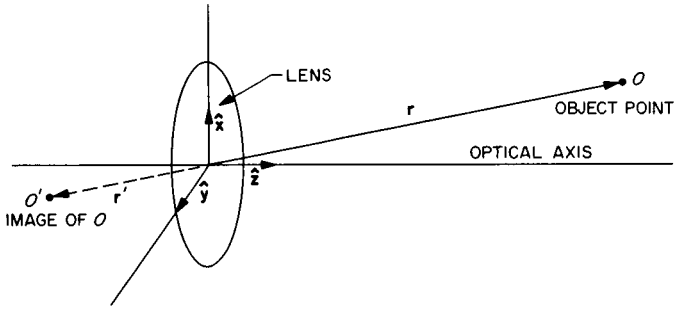

Fig. A-1. Lens-centered coordinate system ($\hat{\mathbf{x}}, \hat{\mathbf{y}}, \hat{\mathbf{z}}$)

Consider the imaging of a single object point. Let an object point O have position vector $\mathbf{r}$ in the lens-centered coordinate system, and let its image O' have a position vector $\mathbf{r}'$ (see Fig. A-1). Then, from similar triangles and the usual refractive properties of thin lenses, one has

$$\mathbf{r}' = \frac{-\mathrm{F}}{\mathbf{r}\cdot\hat{\mathbf{z}} - \mathrm{F}}\,\mathbf{r}$$

where F is the focal length of the lens. If the object distance $\mathbf{r}\cdot\hat{\mathbf{z}}$ is much larger than the focal length, expansion of the above expression gives

$$\mathbf{r}' = \frac{-\mathrm{F}}{\mathbf{r}\cdot\hat{\mathbf{z}}}\mathbf{r}\left(1 + \frac{\mathrm{F}}{\mathbf{r}\cdot\hat{\mathbf{z}}} + \cdots\right)$$

Then, to first order in $\mathrm{F}/\mathbf{r}\cdot\hat{\mathbf{z}}$,

$$\mathbf{r}' \approx -\frac{\mathrm{F}}{\mathbf{r}\cdot\hat{\mathbf{z}}}\mathbf{r}; \qquad \mathbf{r}\cdot\hat{\mathbf{z}} >> \mathrm{F} \tag{A-1}$$

which is the desired result.

Consider next the imaging of an arbitrary straight line segment in space. In the case of distant objects, for a well focused image lying wholly in a plane

parallel to the xy-plane of the lens-centered coordinate system, all points of the line segment must satisfy the condition $\mathbf{r}\cdot\hat{\mathbf{z}} >> \mathrm{F}$ given above for Eq. (A-1). With this provision, let the end points of the object line have position vectors $\mathbf{r}_1$ and $\mathbf{r}_2$, respectively, and let the corresponding image points have position vectors $\mathbf{r}'_1$ and $\mathbf{r}'_2$. From Eq. (A-1), then,

$$\mathbf{r}'_1 = \frac{-\mathrm{F}}{\mathbf{r}_1\cdot\hat{\mathbf{z}}}\mathbf{r}_1$$

and

$$\mathbf{r}'_2 = \frac{-\mathrm{F}}{\mathbf{r}_2\cdot\hat{\mathbf{z}}}\mathbf{r}_2$$

Define the vectors $\mathbf{r}_c$, $\mathbf{R}$, and $\mathbf{R}'$ as follows:

$\mathbf{r}_c = \frac{1}{2}(\mathbf{r}_1 + \mathbf{r}_2)$ the position vector of the object line segment center

$\mathbf{R} = \mathbf{r}_2 - \mathbf{r}_1$ a vector along the object line segment

$\mathbf{R}' = \mathbf{r}'_2 - \mathbf{r}'_1$ a vector along the image line segment

from which it follows that

$$\mathbf{r}_1 = \frac{1}{2}(2\mathbf{r}_c - \mathbf{R})$$

and

$$\mathbf{r}_2 = \frac{1}{2}(2\mathbf{r}_c + \mathbf{R}) \qquad \text{(A-2)}$$

Thus, the vector $\mathbf{R}'$ is written in terms of the object vectors as

$$\mathbf{R}' = \mathrm{F}\left(\frac{\mathbf{r}_1}{\mathbf{r}_1\cdot\hat{\mathbf{z}}} - \frac{\mathbf{r}_2}{\mathbf{r}_2\cdot\hat{\mathbf{z}}}\right) \qquad \text{(A-3)}$$

Substituting Eqs. (A-2) into Eq. (A-3) and collecting terms, one has

$$\mathbf{R}' = 4\mathrm{F}\left[\frac{\mathbf{r}_c(\mathbf{R}\cdot\hat{\mathbf{z}}) - \mathbf{R}(\mathbf{r}_c\cdot\hat{\mathbf{z}})}{4(\mathbf{r}_c\cdot\hat{\mathbf{z}})^2 - (\mathbf{R}\cdot\hat{\mathbf{z}})^2}\right]$$

or

$$\mathbf{R}' = \frac{\mathrm{F}}{(\mathbf{r}_c\cdot\hat{\mathbf{z}})^2}\left[\frac{\hat{\mathbf{z}}\times(\mathbf{r}_c\times\mathbf{R})}{1 - \dfrac{(\mathbf{R}\cdot\hat{\mathbf{z}})^2}{4(\mathbf{r}_c\cdot\hat{\mathbf{z}})^2}}\right] \qquad \text{(A-4)}$$

The condition that all points on the object line segment be very distant from the lens compared to its focal length can be written as

$$\mathbf{r}_c\cdot\hat{\mathbf{z}} - \frac{|\mathbf{R}\cdot\hat{\mathbf{z}}|}{2} >> \mathrm{F}$$

Thus, expanding the right side of Eq. (A-4) and keeping only first-order terms in the small quantities $F/\mathbf{r}_c \cdot \hat{\mathbf{z}}$ and $|\mathbf{R} \cdot \hat{\mathbf{z}}|/2\mathbf{r}_c \cdot \hat{\mathbf{z}}$, one has

$$\mathbf{R}' \approx \frac{F}{(\mathbf{r}_c \cdot \hat{\mathbf{z}})^2} \hat{\mathbf{z}} \times (\mathbf{r}_c \times \mathbf{R}); \qquad \mathbf{r}_c \cdot \hat{\mathbf{z}} - \frac{1}{2}|\mathbf{R} \cdot \hat{\mathbf{z}}| >> F \tag{A-5}$$

which is the desired result for line segments.

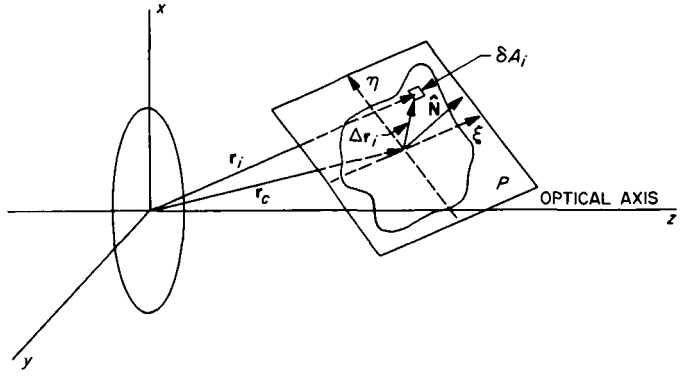

Fig. A-2. Object surface configuration

Next, consider the imaging geometry of an arbitrary plane area for the case in which all points of the area are very distant from a lens compared to the focal length and in which the area occupies a small but finite portion of the field of view. Let the area S lie in a plane P with normal $\hat{\mathbf{N}}$ and have area A_S (see Fig. A-2). Let a Cartesian coordinate system be defined in the plane P with variables ξ and η, so that the area A_S can be written

$$A_S = \iint_S d\xi \, d\eta$$

Without repeating the arguments for convergence, this integral can be written as the limit of a sum, so that

$$A_S = \lim_{N \to \infty} \sum_{i=1}^{N} \delta A_i \tag{A-6}$$

where in the Nth approximation, there are N rectangular elements δA_i covering the region S. Then, writing $\delta A_i'$ and A_S', respectively, as the images of δA_i and A_S, one has, assuming proper convergence,

$$A_S' = \lim_{N \to \infty} \sum_{i=1}^{N} \delta A_i' \tag{A-7}$$

Now, to determine the image of an infinitesimally small plane rectangle δA_i with unit normal $\hat{\mathbf{N}}$, let $\mathbf{R}_1$ and $\mathbf{R}_2$ be vectors along the perpendicular sides of δA_i. Note that $|\mathbf{R}_1|$ and $|\mathbf{R}_2|$ are the lengths of these sides. Let $\mathbf{r}_i$ be the position vector of the center of δA_i, and since $\delta A_i \to 0$, $\mathbf{r}_i$ tends to the position vectors of the centers of the sides $\mathbf{R}_1$ and $\mathbf{R}_2$. Because the whole area S is distant from the

lens compared with the focal length F, Eq. (A-5) applies, giving as the images of $\mathbf{R}_1$ and $\mathbf{R}_2$ the vectors $\mathbf{R}'_1$ and $\mathbf{R}'_2$, where

$$\mathbf{R}'_1 = \frac{F}{(\mathbf{r}_i \cdot \hat{\mathbf{z}})^2} \hat{\mathbf{z}} \times (\mathbf{r}_i \times \mathbf{R}_1)$$

and

$$\mathbf{R}'_2 = \frac{F}{(\mathbf{r}_i \cdot \hat{\mathbf{z}})^2} \hat{\mathbf{z}} \times (\mathbf{r}_i \times \mathbf{R}_2)$$

Both δA_i and $\delta A'_i$ are parallelograms; hence, with the above assumptions,

$$\delta A_i = |\mathbf{R}_1 \times \mathbf{R}_2|$$

and

$$\delta A'_i = |\mathbf{R}'_1 \times \mathbf{R}'_2|$$

Calculating $\delta A'_i$,

$$\mathbf{R}'_1 \times \mathbf{R}'_2 = \frac{F^2}{(\mathbf{r}_i \cdot \hat{\mathbf{z}})^4} [\hat{\mathbf{z}} \times (\mathbf{r}_i \times \mathbf{R}_1)] \times [\hat{\mathbf{z}} \times (\mathbf{r}_i \times \mathbf{R}_2)]$$

or

$$\mathbf{R}'_1 \times \mathbf{R}'_2 = \frac{F^2}{(\mathbf{r}_i \cdot \hat{\mathbf{z}})^3} \{\mathbf{R}_1 \times \mathbf{R}_2 (\mathbf{r}_i \cdot \hat{\mathbf{z}}) + \mathbf{r}_i \times [\hat{\mathbf{z}} \times (\mathbf{R}_1 \times \mathbf{R}_2)]\}$$

where the vector identity $\mathbf{A} \times (\mathbf{B} \times \mathbf{C}) = \mathbf{B}(\mathbf{A} \cdot \mathbf{C}) - \mathbf{C}(\mathbf{A} \cdot \mathbf{B})$ for arbitrary vectors **A**, **B**, and **C** has been used. It is further noted that $\mathbf{R}_1 \times \mathbf{R}_2 = \pm |\mathbf{R}_1 \times \mathbf{R}_2| \hat{\mathbf{N}}$, the sign depending on specific orientations but of no consequence. Substituting this in the above and expanding and collecting terms, one has

$$\mathbf{R}'_1 \times \mathbf{R}'_2 = \pm \frac{F^2 (\mathbf{r}_i \cdot \hat{\mathbf{N}})}{(\mathbf{r}_i \cdot \hat{\mathbf{z}})^3} |\mathbf{R}_1 \times \mathbf{R}_2| \hat{\mathbf{z}}$$

and finally,

$$\delta A'_i = F^2 \left| \frac{\mathbf{r}_i \cdot \hat{\mathbf{N}}}{(\mathbf{r}_i \cdot \hat{\mathbf{z}})^3} \right| \delta A_i \tag{A-8}$$

Substitution of Eq. (A-8) in Eq. (A-7) gives

$$A'_S = \lim_{N \to \infty} \sum_{i=1}^{N} F^2 \left| \frac{\mathbf{r}_i \cdot \hat{\mathbf{N}}}{(\mathbf{r}_i \cdot \hat{\mathbf{z}})^3} \right| \delta A_i \tag{A-9}$$

The sum in Eq. (A-9) is approximated as follows. Let $\mathbf{r}_c$ be the position vector of the areal center of *S*. That is, let

$$\mathbf{r}_c = \frac{1}{A_S} \iint_S \mathbf{r} \, d\xi \, d\eta \tag{A-10}$$

where $\mathbf{r}$ is the position vector of the element $d\xi\, d\eta$. Then, define $\Delta\mathbf{r}_i$ such that $\mathbf{r}_i = \mathbf{r}_c + \Delta\mathbf{r}_i$ (see Fig. A-2). Since by hypothesis, the area S is everywhere distant from the lens compared with the focal length, or

$$\mathbf{r}_c \cdot \hat{\mathbf{z}} - |\Delta\mathbf{r}_i \cdot \hat{\mathbf{z}}| >> \mathrm{F} \qquad \text{for all } i$$

one has

$$\frac{1}{|\mathbf{r}_i \cdot \hat{\mathbf{z}}|^3} = \frac{1}{|\mathbf{r}_c \cdot \hat{\mathbf{z}}|^3}\left|1 - 3\frac{\Delta\mathbf{r}_i \cdot \hat{\mathbf{z}}}{\mathbf{r}_c \cdot \hat{\mathbf{z}}} + \cdots\right| \approx \frac{1}{|\mathbf{r}_c \cdot \hat{\mathbf{z}}|^3}$$

keeping only zeroth order in $\Delta\mathbf{r}_i \cdot \hat{\mathbf{z}}/\mathbf{r}_c \cdot \hat{\mathbf{z}}$. Furthermore, assume that $\mathbf{r}_i \cdot \hat{\mathbf{N}}$ is either positive for all i or negative for all i, since the surface being imaged can always be separated into two parts, each satisfying one of these conditions, and each part can be treated separately. Then, Eq. (A-9) can be rewritten as

$$A'_S \approx \frac{\mathrm{F}^2}{|\mathbf{r}_c \cdot \mathbf{z}|^3} \lim_{N\to\infty}\left|\sum_{i=1}^{N} (\mathbf{r}_i \cdot \hat{\mathbf{N}})\, \delta A_i\right|$$

or

$$A'_S \approx \frac{\mathrm{F}^2}{|\mathbf{r}_c \cdot \hat{\mathbf{z}}|^3}\left|\hat{\mathbf{N}} \cdot \iint_S \mathbf{r}\, d\xi\, d\eta\right|$$

and using definition (A-10),

$$A'_S \approx \frac{\mathrm{F}^2\, |\mathbf{r}_c \cdot \hat{\mathbf{N}}|}{|\mathbf{r}_c \cdot \hat{\mathbf{z}}|^3} A_S \tag{A-11}$$

which is the desired result.

APPENDIX B

Two-Dimensional Linear System Analysis and Application to Television Systems

In this Appendix is considered the extension to two-dimensional systems of the familiar Fourier transform treatment of linear one-dimensional systems as, for example, the treatment of time-dependent electrical signals passing through linear circuitry. The results are then specialized to be applied to scanning television systems.

Consider a general two-dimensional transfer system in which an input stimulus array $i(x, y)$ is processed through the system to a response array $r(\xi, \eta)$, where the coordinate pair (ξ, η) of the output is some function of the coordinate pair (x, y) of the input. The action of the system on the input can be thought of as some operation $F[\ ]$, so that for an input $i(x, y)$, the output $r(\xi, \eta)$ is given by

$$r(\xi, \eta) = F[i(x, y)]$$

Such a system is said to be *linear* if for two arbitrary input arrays $i_1(x, y)$ and $i_2(x, y)$ and for arbitrary constants a and b, the outputs corresponding to the inputs $ai_1(x, y)$ and $ai_1(x, y) + bi_2(x, y)$ are given, respectively, by

$$r(\xi, \eta) = F[ai_1(x, y)] = aF[i_1(x, y)]$$

and

$$r(\xi, \eta) = F[ai_1(x, y) + bi_2(x, y)] = aF[i_1(x, y)] + bF[i_2(x, y)]$$

Obviously, such a linear operation can have a wide variety of forms as, for example, forming a simple linear function of the input, differentiating the input, or integrating the input.

In treating such a system analytically, it is most convenient to use a sum or integral representation for the arbitrary input to exploit the linearity properties to their fullest. As an example and as an obvious first candidate for such a representation, consider the Fourier integral (note that the Fourier series can be written as a special case of the integral). The convention will be adopted that the function being transformed will be denoted by a lower-case letter and its transform by an upper case letter. So, if $i(x, y)$ is some input function and $I(k_x, k_y)$ is its Fourier transform,

$$i(x, y) = \int_{-\infty}^{\infty} dk_x \int_{-\infty}^{\infty} dk_y\, I(k_x, k_y) \exp[i(k_x x + k_y y)]$$

and

$$I(k_x, k_y) = \frac{1}{(2\pi)^2} \int_{-\infty}^{\infty} dx \int_{-\infty}^{\infty} dy\, i(x, y) \exp[-i(k_x x + k_y y)]$$

where it is assumed that both functions exist. The usefulness of such a representation is readily apparent upon noting that it is a linear combination of standard

inputs of the form $\exp[i(k_x x + k_y y)]$. Thus, the action of the linear system operator $F[\ ]$ on the input $i(x, y)$ gives an output $r(\xi, \eta)$, where

$$r(\xi, \eta) = F\left[\int_{-\infty}^{\infty} dk_x \int_{-\infty}^{\infty} dk_y\, I(k_x, k_y) \exp\{i(k_x x + k_y y)\}\right]$$

or

$$r(\xi, \eta) = \int_{-\infty}^{\infty} dk_x \int_{-\infty}^{\infty} dk_y\, I(k_x, k_y)\, F[\exp\{i(k_x x + k_y y)\}] \tag{B-1}$$

having imposed the linearity property of the system. Thus, to specify completely the action of the system on any arbitrary input $i(x, y)$ whose Fourier transform exists, one need only know its effect on the general two-dimensional sinusoidal input $\exp[i(k_x x + k_y y)]$ as a function of the "frequencies" k_x and k_y. Note that the usefulness of an integral expansion lies in the fact that the response of the system to an arbitrary input is determined by the response of the system to each of a set of standard functions in terms of which the input is written. The set of standard functions can be chosen for the convenience of the problem at hand.

In the application of such a formalism to scanning television systems, obviously the major obstacle to overcome is the condition of linearity which must be imposed. Overall linearity depends to a very large extent upon the characteristics of each individual system being considered and so cannot be accounted for with any great generality. In the limit of "small enough" input amplitudes, however, one can assume linearity in that the system transfer function will have only significant constant and first-derivative terms in its Taylor's series expansion with respect to input amplitude about the mean input level. Note that the term, small enough, is tacitly defined in such a way as to guarantee negligible terms in higher-order derivatives than the first.

Assuming, then, that one is in fact dealing with a linear television system,at least to some degree of approximation, the above general linear system formalism can be specialized as follows. It seems convenient to use the Fourier integral representation, so that the standard input function is taken as a spatial sine-wave luminance distribution over the field of view of the camera of the form $\exp[i(k_x x + k_y y)]$. The resulting output can be calculated straightforwardly from scanning theory, again assuming certain linearity conditions to which the previous comments on linearity apply. Such a calculation indicates that the output is a sinusoidal distribution with spatial frequencies that are functions of the input frequencies but have altered phase and amplitude. This result can be written as

$$\begin{aligned} r(\xi, \eta) &= F[\exp\{i(k_x x + k_y y)\}] \\ &= A(x, y)\, G(x, y, k_x, k_y) \exp[i(k_x x + k_y y)] \end{aligned} \tag{B-2}$$

where $\xi = \xi(x, y)$, $\eta = \eta(x, y)$, and the spatial frequencies k_x and k_y transform to k_ξ and k_η such that for corresponding points (ξ, η) and (x, y), one has

$$(k_x x + k_y y) = (k_\xi \xi + k_\eta \eta)$$

Furthermore, $G(x, y, k_x, k_y)$ is the system sine-wave response or modulation transfer function (in general complex) normalized such that $G(x, y, 0, 0) \equiv 1$ and $A(x, y)$ is an amplitude transfer factor independent of frequency. Note that the

functions $\xi(x, y)$ and $\eta(x, y)$ can account for geometrical distortions between the input and output, and the function $A(x, y)\, G(x, y, k_x, k_y)$ can account for response nonuniformities and scan-line structure.

Using Eq. (B-1), then, the response $r(\xi, \eta)$ to an input $i(x, y)$ which has a Fourier transform $I(k_x, k_y)$ is

$$r(\xi, \eta) = A(x, y) \int_{-\infty}^{\infty} dk_x \int_{-\infty}^{\infty} dk_y\, I(k_x, k_y)\, G(x, y, k_x, k_y) \exp[i(k_x x + k_y y)] \quad \text{(B-3)}$$

It is sometimes convenient to rework Eq. (B-3) in the form of a convolution integral. This is readily accomplished with the following manipulations. The transform pairs involved are

$$i(x, y) = \int_{-\infty}^{\infty} dk_x \int_{-\infty}^{\infty} dk_y\, I(k_x, k_y) \exp[i(k_x x + k_y y)]$$

$$I(k_x, k_y) = \frac{1}{(2\pi)^2} \int_{-\infty}^{\infty} dx \int_{-\infty}^{\infty} dy\, i(x, y) \exp[-i(k_x x + k_y y)]$$

and

$$g(x, y, \upsilon, v) = \int_{-\infty}^{\infty} dk_\upsilon \int_{-\infty}^{\infty} dk_v\, G(x, y, k_\upsilon, k_v) \exp[i(k_\upsilon \upsilon + k_v v)]$$

$$G(x, y, k_\upsilon, k_v) = \frac{1}{(2\pi)^2} \int_{-\infty}^{\infty} d\upsilon \int_{-\infty}^{\infty} dv\, g(x, y, \upsilon, v) \exp[-i(k_\upsilon \upsilon + k_v v)]$$

Substituting in Eq. (B-3) for these quantities, one has

$$r(\xi, \eta) = \frac{A(x, y)}{(2\pi)^4} \int_{-\infty}^{\infty} dk_x \int_{-\infty}^{\infty} dk_y \int_{-\infty}^{\infty} dx' \int_{-\infty}^{\infty} dy' \int_{-\infty}^{\infty} d\upsilon \int_{-\infty}^{\infty} dv\, i(x', y')\, g(x, y, \upsilon, v) \exp[ik_x(x - x' - \upsilon) \times \exp[ik_y(y - y' - v)]$$

Thus, noting the familiar representation for the Dirac delta function,

$$\delta(x) = \frac{1}{2\pi} \int_{-\infty}^{\infty} dk \exp(ikx)$$

this can be rewritten as

$$r(\xi, \eta) = \frac{A(x, y)}{(2\pi)^2} \int_{-\infty}^{\infty} dx' \int_{-\infty}^{\infty} dy' \int_{-\infty}^{\infty} d\upsilon \int_{-\infty}^{\infty} dv\, i(x', y')\, g(x, y, \upsilon, v)\, \delta(x - x' - \upsilon)\, \delta(y - y' - v) \quad \text{(B-4)}$$

Equation (B-4) can be further reduced in various ways to give four equally valid forms for the two-dimensional convolution integral representation for the response $r(\xi, \eta)$ in terms of the input $i(x, y)$. One of these is given below, the others being trivial permutations:

$$r(\xi, \eta) = \frac{A(x, y)}{(2\pi)^2} \int_{-\infty}^{\infty} d\upsilon \int_{-\infty}^{\infty} dv\, i(x - \upsilon, y - v)\, g(x, y, \upsilon, v) \quad \text{(B-5)}$$

APPENDIX C

System Noise in the Output Film

In computing the signal-to-noise ratio in the system output, one needs to know the root-mean-square transmission variations about the local mean. This quantity is most easily determined experimentally with a scanning microphotometer. Thus, in this Appendix, the rms noise in the output transparency is determined in terms of the output of a scanning microphotometer.

Let $t(\xi, \eta)$ be the noisy reproduction of a spatially uniform input luminance distribution, where $t(\xi, \eta)$ includes the scan-line structure due to the television process. In a manner similar to that discussed in Appendix B, $t(\xi, \eta)$ can be written from scanning theory as

$$t(\xi, \eta) = t_0 + s(\xi, \eta)[t_1 + t_N(\xi, \eta)] \tag{C-1}$$

where t_0 is the base film transmission, $s(\xi, \eta)$ is a function accounting for scan-line structure, t_1 is a constant, and $t_N(\xi, \eta)$ is the superimposed transmission noise. Note that the spatial averages of $s(\xi, \eta)$ and $t_N(\xi, \eta)$ are taken to be 1 and 0, respectively, but that the amplitudes of their fluctuations about the averages as well as the value of the constant t_1 depend upon the input luminance level.

If one assigns a spatial frequency distribution $T_N(k_\xi, k_\eta)$, to the noise portion $t_N(\xi, \eta)$, $t_N(\xi, \eta)$ can be written in its Fourier representation simply as

$$t_N(\xi, \eta) = \int_{-\infty}^{\infty} dk_\xi \int_{-\infty}^{\infty} dk_\eta \, T_N(k_\xi, k_\eta) \exp\{i[k_\xi \xi + k_\eta \eta + \phi(k_\xi, k_\eta)]\} \tag{C-2}$$

where for all spatial frequencies k_ξ and k_η, $\phi(k_\xi, k_\eta)$ is a real random variable uniformly distributed over 2π. It is useful to note certain results of the condition that $t_N(\xi, \eta)$ is a real function. Namely, if * denotes a complex conjugate, for $t_N(\xi, \eta) = t_N^*(\xi, \eta)$,

$$\int_{-\infty}^{\infty} dk_\xi \int_{-\infty}^{\infty} dk_\eta \, T_N(k_\xi, k_\eta) \exp\{i[k_\xi \xi + k_\eta \eta + \phi(k_\xi, k_\eta)]\} = \int_{-\infty}^{\infty} dk_\xi \int_{-\infty}^{\infty} dk_\eta \, T_N(k_\xi, k_\eta) \exp\{-i[k_\xi \xi + k_\eta \eta + \phi(k_\xi, k_\eta)]\}$$

Then, making the transformation $k_\xi \to -k_\xi$ and $k_\eta \to -k_\eta$ in the second integral, it follows that

$$\int_{-\infty}^{\infty} dk_\xi \int_{-\infty}^{\infty} dk_\eta \, T_N(k_\xi, k_\eta) \exp\{i[k_\xi \xi + k_\eta \eta + \phi(k_\xi, k_\eta)]\}$$
$$= \int_{-\infty}^{\infty} dk_\xi \int_{-\infty}^{\infty} dk_\eta \, T_N(-k_\xi, -k_\eta) \exp\{i[k_\xi \xi + k_\eta \eta - \phi(-k_\xi, -k_\eta)]\}$$

for any physically realizable spectral distribution or phase function. So, the desired consequences of the reality of $t_N(\xi, \eta)$ are that

$$T_N(k_\xi, k_\eta) = T_N(-k_\xi, -k_\eta)$$

and

$$\phi(k_\xi, k_\eta) = -\phi(-k_\xi, -k_\eta) \tag{C-3}$$

The desired information about the noise lies in the values of the spatial averages of $t(\xi, \eta)$ and $t^2(\xi, \eta)$. Consider first the average of $t(\xi, \eta)$ or $\langle t(\xi, \eta)\rangle$. Since averaging is a linear process, from Eq. (C-1),

$$\langle t(\xi, \eta)\rangle = t_0 + t_1 \langle s(\xi, \eta)\rangle + \langle s(\xi, \eta)\, t_N(\xi, \eta)\rangle$$

As defined earlier, the normalization of $s(\xi, \eta)$ is such that $\langle s(\xi, \eta)\rangle = 1$. Also, the third term vanishes since the spatial average can be broken into averages along strips taken parallel to the scan lines and then an average over these strips. The averages along the strips all vanish since $s(\xi, \eta)$ is constant along a strip parallel to the scan lines and $\langle t_N(\xi, \eta)\rangle = 0$, since $t_N(\xi, \eta)$ is assumed to be an isotropic function of position, so that the whole average $\langle s(\xi, \eta)\, t_N(\xi, \eta)\rangle$ vanishes. Thus, the average transmission of the noisy image of a uniform field is

$$\langle t(\xi, \eta)\rangle = t_0 + t_1 \tag{C-4}$$

Finally, consider the average of $t^2(\xi, \eta)$ or $\langle t^2(\xi, \eta)\rangle$. From Eq. (C-1), one has

$$\langle t^2(\xi, \eta)\rangle = t_0^2 + t_1^2 \langle s^2(\xi, \eta)\rangle + \langle s^2(\xi, \eta)\, t_N^2(\xi, \eta)\rangle + 2t_0 t_1 \langle s(\xi, \eta)\rangle + 2t_0 \langle s(\xi, \eta)\, t_N(\xi, \eta)\rangle + 2t_1 \langle s^2(\xi, \eta)\, t_N(\xi, \eta)\rangle$$

Now, by the above arguments, several terms vanish and straightforward averages are evaluated, so that

$$\langle t^2(\xi, \eta)\rangle = t_0^2 + 2t_0 t_1 + t_1^2 \langle s^2(\xi, \eta)\rangle + \langle s^2(\xi, \eta)\, t_N^2(\xi, \eta)\rangle$$

Furthermore, by the same arguments, the last term can be broken into two averages; thus,

$$\langle s^2(\xi, \eta)\, t_N^2(\xi, \eta)\rangle = \langle s^2(\xi, \eta)\rangle \langle t_N^2(\xi, \eta)\rangle$$

Note that this result also follows from the Fourier integral representations for $s(\xi, \eta)$ and $t_N(\xi, \eta)$, remembering that $\phi(k_\xi, k_\eta)$ in the representation of $t_N(\xi, \eta)$ is a random variable. In any case, one has

$$\langle t^2(\xi, \eta)\rangle = t_0^2 + 2t_0 t_1 + t_1^2 \langle s^2(\xi, \eta)\rangle + \langle s^2(\xi, \eta)\rangle \langle t_N^2(\xi, \eta)\rangle \tag{C-5}$$

It is useful to write the averages $\langle s^2(\xi, \eta)\rangle$ and $\langle t_N^2(\xi, \eta)\rangle$ in terms of their Fourier transformations. First of all, $s(\xi, \eta)$, representing the scan-line structure, is a periodic function of one direction only and constant in the other. Let the η-axis be normal to the scan lines, so that $s(\xi, \eta) = s(\eta)$, and let the scan lines be periodic in a distance ρ. Then, $s(\eta)$ can be written as

$$s(\eta) = \sum_{k=-\infty}^{\infty} A_k \exp\left(2\pi i \frac{k\eta}{\rho}\right)$$

where

$$A_k = \frac{1}{\rho}\int_{-\rho/2}^{\rho/2} s(\eta) \exp\left(-2\pi i \frac{k\eta}{\rho}\right) d\eta$$

Thus, it follows that

$$\langle s^2(\xi, \eta)\rangle = \frac{1}{\rho}\int_{-\rho/2}^{\rho/2} \sum_{k,\,l} A_k A_l \exp\left[2\pi i \frac{\eta(k+l)}{\rho}\right] d\eta = \sum_{k=-\infty}^{\infty} A_k A_{-k}$$

Since $s(\xi, \eta)$ is a real function, it follows that $A_{-k} = A_k^*$, so that

$$\langle s^2(\xi, \eta)\rangle = \sum_{k=-\infty}^{\infty} |A_k|^2 = |A_0|^2 + 2\sum_{k=1}^{\infty} |A_k|^2 \tag{C-6}$$

Similarly, the average $\langle t_N^2(\xi,\eta)\rangle$ is calculated, using Eq. (C-2), as

$$\langle t_N^2(\xi,\eta)\rangle = \lim_{a,b\to\infty}\frac{1}{ab}\int_{-a/2}^{a/2}d\xi\int_{-b/2}^{b/2}d\eta\int_{-\infty}^{\infty}dk_\xi\int_{-\infty}^{\infty}dk_\eta\int_{-\infty}^{\infty}dk'_\xi\int_{-\infty}^{\infty}dk'_\eta\,T_N(k_\xi,k_\eta)\,T_N(k'_\xi,k'_\eta)$$
$$\times\exp\{i[(k_\xi+k'_\xi)\xi+(k_\eta+k'_\eta)\eta+\phi(k_\xi,k_\eta)+\phi(k'_\xi,k'_\eta)]\}$$

Then, being somewhat lax about limits, it follows that

$$\langle t_N^2(\xi,\eta)\rangle = \int_{-\infty}^{\infty}dk_\xi\int_{-\infty}^{\infty}dk_\eta\,T_N(k_\xi,k_\eta)\,T_N(-k_\xi,-k_\eta)\exp\{i[\phi(k_\xi,k_\eta)+\phi(-k_\xi,-k_\eta)]\}$$

and, using Eq. (C-3), one finally has

$$\langle t_N^2(\xi,\eta)\rangle = \int_{-\infty}^{\infty}dk_\xi\int_{-\infty}^{\infty}dk_\eta\,|T_N(k_\xi,k_\eta)|^2 \tag{C-7}$$

Now, having calculated $\langle t(\xi,\eta)\rangle$ and $\langle t^2(\xi,\eta)\rangle$, one finds the rms noise variations $\langle t_N\rangle_{\rm rms}$ as follows. By definition,

$$\langle t_N\rangle_{rms}^2 = \langle[t(\xi,\eta)-\langle t(\xi,\eta)\rangle]^2\rangle = \langle t^2(\xi,\eta)\rangle - \langle t(\xi,\eta)\rangle^2$$

So, from Eqs. (C-4) and (C-5),

$$\langle t_N\rangle_{\rm rms}^2 = t_1^2[\langle s^2(\xi,\eta)\rangle - 1] + \langle s^2(\xi,\eta)\rangle\langle t_N^2(\xi,\eta)\rangle \tag{C-8}$$

In the Fourier representation, then, noting that $\langle s(\xi,\eta)\rangle = 1$ implies from

$$\langle s(\xi,\eta)\rangle = \sum_{k=-\infty}^{\infty}A_k\left\langle\exp\left(2\pi i\frac{k\eta}{\rho}\right)\right\rangle = A_0$$

that $A_0 = 1$, one has

$$\langle t_N\rangle_{\rm rms}^2 = 2t_1^2\sum_{k=1}^{\infty}|A_k|^2 + \sum_{k=-\infty}^{\infty}|A_k|^2\int_{-\infty}^{\infty}dk_\xi\int_{-\infty}^{\infty}dk_\eta\,|T_N(k_\xi,k_\eta)|^2 \tag{C-9}$$

which is the desired result.

As mentioned earlier, it remains only to determine the various constants in the expression for the transmission (see Eq. C-1) and the amplitudes of the scan-line and noise fluctuations. Given these, $\langle t_N\rangle_{\rm rms}$ can be computed from Eq. (C-9). To measure the required parameters, consider the output of a scanning microphotometer. For simplicity, let the aperture be rectangular, with dimensions d_1 and d_2, and let the aperture orientation be as shown in Fig. C-1, with the sides parallel to the ξ- and η-axes. Let a (u,w)-coordinate system be located with its origin at the center of the aperture and with its axes parallel to the (ξ,η)-axes. Finally, let the center of the aperture move with velocity components v_ξ and v_η in the (ξ,η)-coordinate system. A point with coordinates (u,w) in the aperture coordinate system has coordinates $(u+v_\xi\tau, w+v_\eta\tau)$ in the (ξ,η)-system at time τ. Then, since the microphotometer measures the average transmission over the aperture, the output $t^a(\tau)$ at a particular time τ is given by

$$t^a(\tau) = \langle t(u+v_\xi\tau, w+v_\eta\tau)\rangle_a = t_0 + t_1\langle s(w+v_\eta\tau)\rangle_a + \langle s(w+v_\eta\tau)\,t_N(u+v_\xi\tau, w+v_\eta\tau)\rangle_a$$

where $t(\xi,\eta)$ is the noisy transmission distribution given in Eq. (C-1), and the average of $t(\xi,\eta)$ over the aperture $\langle t(u+v_\xi\tau, w+v_\eta\tau)\rangle_a$ is given by

$$\langle t(u+v_\xi\tau, w+v_\eta\tau)\rangle_a = \frac{1}{d_1d_2}\int_{-d_1/2}^{d_1/2}du\int_{-d_2/2}^{d_2/2}dw\,t(u+v_\xi\tau, w+v_\eta\tau)$$

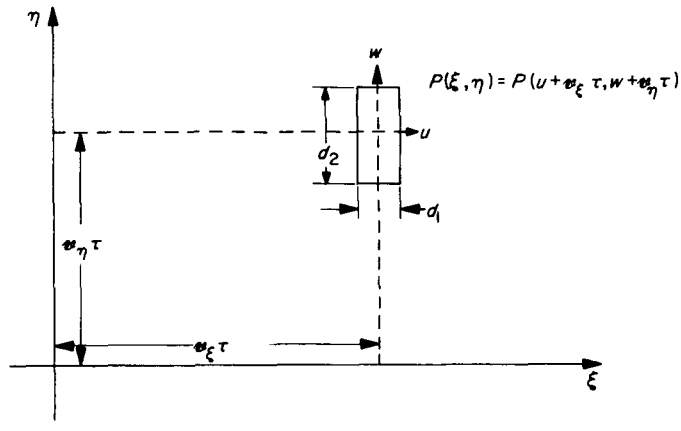

Fig. C-1. Scanning-aperture geometry

Using the Fourier representation for the various terms in $t(\xi, \eta)$, $t^a(\tau)$ becomes, after some calculation,

$$t^a(\tau) = t_0 + \frac{t_1\rho}{\pi d_2} \sum_{m=-\infty}^{\infty} A_m \frac{\sin \frac{\pi m d_2}{\rho}}{m} \exp\left(2\pi i \frac{m v_\eta \tau}{\rho}\right) + \frac{4}{d_1 d_2} \sum_{m=-\infty}^{\infty} \int_{-\infty}^{\infty} dk_\xi \int_{-\infty}^{\infty} dk_\eta A_m T_N(k_\xi, k_\eta)$$

$$\times \exp\left[i\phi(k\xi, k_\eta)\right] \frac{\sin k_\xi \frac{d_1}{2}}{k_\xi} \frac{\sin\left(\frac{2\pi m}{\rho} + k_\eta\right)\frac{d_2}{2}}{\frac{2\pi m}{\rho} + k_\eta} \exp\left\{i\left[k_\xi v_\xi + \left(\frac{2\pi m}{\rho} + k_\eta\right) v_\eta\right]\tau\right\} \qquad \text{(C-10)}$$

Then, if $v_\eta \neq 0$, it follows that

$$\langle t^a(\tau)\rangle = \lim_{\tau_0 \to \infty} \frac{1}{\tau_0} \int_{-\tau_0/2}^{\tau_0/2} t(\tau)\, d\tau$$

is simply

$$\langle t^a(\tau)\rangle = t_0 + t_1 A_0 = t_0 + t_1 \qquad \text{(C-11)}$$

where it is recalled that $\langle s(\xi, \eta)\rangle = 1$ implies that $A_0 = 1$. Obviously, the larger the scanning aperture, the faster $\langle t(\tau)\rangle$ converges in time, since the functions of the form $\sin ax/ax$ (a is related linearly to the aperture dimension and x to the spatial frequency) exhibit a progressively sharper peak about $x = 0$ for increasingly larger a.

The shape and amplitude of the scan-line function can be determined simply by scanning only in the direction normal to the scan lines ($v_\xi = 0$), with an aperture having d_1 as large as possible and $d_2 << \rho$, the periodicity dimension of the scan lines. Making d_1 large greatly reduces the amplitude of the random noise term in Eq. (C-10), and if $d_2 << \rho$, the factor $\sin(\pi m d_2/\rho)/(\pi m d_2/\rho)$ is very nearly unity for $|m| << \rho/d_2$, which is a large number. However, the amplitudes A_m become small for rather small $|m|$, so that making $d_2 << \rho$ guarantees a good reproduction of the signficant sine-wave components of $s(\eta)$ and, hence, of $s(\eta)$ itself. Thus, averaging out what remains of the random noise,

a trace normal to the scan lines with an aperture of appropriate dimensions gives as the time-dependent output from the microphotometer

$$t^a(\tau) \approx t_0 + t_1 s(v_\eta \tau) \tag{C-12}$$

which follows directly from Eq. (C-10) and the Fourier representation of $s(\eta)$. From this output, the shape and amplitude of the scan-line structure can be determined.

Finally, given some shape for the noise spectrum, it remains to determine its absolute normalization. Let $T_0 T_N(k_x, k_y)$ be the complete spectral distribution of the noise, where $T_N(k_x, k_y)$ is a function with fixed normalization determining the shape of the spectrum and T_0 is a constant determining the absolute normalization. Now, let the film be scanned in the direction parallel to the scan lines, with an aperture having dimension d_2 normal to the scan lines which is very small compared to the scan-line periodicity dimension ρ. Then, if the position of the center of the aperture is $(v_\xi \tau, \eta_0)$, the microphotometer output is

$$t^a(\tau) = t_0 + t_1 s(\eta_0) + s(\eta_0) \langle t_N(u + v_\xi \tau, w + \eta_0) \rangle_a$$

and

$$[t^a(\tau)]^2 = t_0^2 + t_1^2 s^2(\eta_0) + s^2(\eta_0) \langle t_N(u + v_\xi \tau, w + \eta_0) \rangle_a^2 + 2t_0 t_1 s(\eta_0) + 2t_0 s(\eta_0) \langle t_N(u + v_\xi \tau, w + \eta_0 \rangle_a + 2t_1 s^2(\eta_0) \langle t_N(u + v_\xi \tau, w + \eta_0) \rangle_a$$

Using the previous arguments, the averages $\langle t^a(\tau) \rangle$ and $\langle (t^a)^2(\tau) \rangle$ can be computed as

$$\langle t^a(\tau) \rangle = t_0 + t_1 s(\eta_0)$$

and

$$\langle [t^a(\tau)]^2 \rangle = t_0^2 + 2t_0 t_1 s(\eta_0) + t_1^2 s^2(\eta_0) + s^2(\eta_0) \langle \langle t_N(u + v_\xi \tau, w + \eta_0 \rangle_a^2 \rangle$$

so that the square of the rms microphotometer output noise $\langle t_N^a \rangle_{\text{rms}}$ is

$$\langle t_N^a \rangle_{\text{rms}}^2 = \langle [t^a(\tau)]^2 \rangle - \langle t^a(\tau) \rangle^2 = s^2(\eta_0) \langle \langle t_N(u + v_\xi \tau, w + \eta_0) \rangle_a^2 \rangle$$

Now,

$$\langle t_N(u + v_\xi \tau, w + \eta_0) \rangle_a = \frac{T_0}{d_1 d_2} \int_{-d_1/2}^{d_1/2} du \int_{-d_2/2}^{d_2/2} dw \int_{-\infty}^{\infty} dk_\xi \int_{-\infty}^{\infty} dk_\eta T_N(k_\xi, k_\eta) \exp\{i[k_\xi(u + v_\xi \tau) + k_\eta(w + \eta_0) + \phi(k_\xi, k_\eta)]\}$$

from which it follows that

$$\langle t_N(u + v_\xi \tau, w + \eta_0) \rangle_a^2 = \frac{T_0^2}{(d_1 d_2)^2} \int_{-d_1/2}^{d_1/2} du \int_{-d_2/2}^{d_2/2} dw \int_{-d_1/2}^{d_1/2} du' \int_{-d_2/2}^{d_2/2} dw' \int_{-\infty}^{\infty} dk_\xi \int_{-\infty}^{\infty} dk_\eta \int_{-\infty}^{\infty} dk'_\xi \int_{-\infty}^{\infty} dk'_\eta$$
$$\times T_N(k_\xi, k_\eta) T_N(k'_\xi, k'_\eta) \exp\{i[k_\xi u + k'_\xi u' + k_\eta(w + \eta_0) + k'_\eta(w' + \eta_0)]\}$$
$$\times \exp\{i[(k_\xi + k'_\xi) v_\xi \tau + \phi(k_\xi, k_\eta) + \phi(k'_\xi, k'_\eta)]\}$$

and, finally,

$$\langle\langle t_N(u + v_\xi\tau, w + \eta_0)\rangle_a^2\rangle = \left(\frac{4T_0}{d_1d_2}\right)^2 \int_{-\infty}^{\infty} dk_\xi \int_{-\infty}^{\infty} dk_\eta \, |T_N(k_\xi, k_\eta)|^2 \frac{\sin^2 \frac{k_\xi d_1}{2}}{k_\xi^2} \frac{\sin^2 \frac{k_\eta d_2}{2}}{k_\eta^2}$$

Therefore,

$$\langle t_N^a\rangle_{\text{rms}}^2 = s^2(\eta_0)\left(\frac{4T_0}{d_1d_2}\right)^2 \int_{-\infty}^{\infty} dk_\xi \int_{-\infty}^{\infty} dk_\eta \, |T_N(k_\xi, k_\eta)|^2 \frac{\sin^2 \frac{k_\xi d_1}{2}}{k_\xi^2} \frac{\sin^2 \frac{k_\eta d_2}{2}}{k_\eta^2} \quad \text{(C-13)}$$

from which the normalization constant T_0 can be determined, given the general spectrum shape $T_N(k_\xi, k_\eta)$. Hence, the information needed in computing $\langle t_N\rangle_{\text{rms}}^2$ in Eq. (C-9) can be obtained simply from the film under consideration with a scanning microphotometer.

ACKNOWLEDGMENTS

The evolution of the figure of merit to its present form has taken place over several years. During that time, the development of its various aspects has been aided by helpful discussions with numerous people at the Jet Propulsion Laboratory. In particular, Mr. Gerald M. Smith has given continuing encouragement and has taken part in many of these discussions. The authors gratefully acknowledge these contributions.